The Plant Journal (2005) **42**, 844–861 doi: 10.1111/j.1365-313X.2005.02418.x

Characterization of two *GL8* paralogs reveals that the 3-ketoacyl reductase component of fatty acid elongase is essential for maize (*Zea mays* L.) development

Charles R. Dietrich[1,2,†], M. Ann D. N. Perera[2,3], Marna D. Yandeau-Nelson[1,4], Robert B. Meeley[5], Basil J. Nikolau[2,3,6,7] and Patrick S. Schnable[1,2,4,6,7,8,*]

[1]*Department of Genetics, Development and Cell Biology,*
[2]*Interdepartmental Plant Physiology Program,*
[3]*Department of Biochemistry, Biophysics and Molecular Biology,*
[4]*Interdepartmental Genetics Program,*
[5]*Pioneer Hi-Bred International, Inc.*
[6]*Center for Plant Genomics,*
[7]*Center for Designer Crops and*
[8]*Department of Agronomy, Iowa State University, Ames, IA 50011, USA*

Received 19 November 2004; revised 8 March 2005; accepted 15 March 2005.
[*]For correspondence (fax 515 294 5256; e-mail schnable@iastate.edu).
[†]Present address: USDA-ARS Plant Genetics Research Unit, St Louis, MO 63132, USA.

Summary

Prior analyses established that the maize (*Zea mays* L.) *gl8a* gene encodes 3-ketoacyl reductase, a component of the fatty acid elongase required for the biosynthesis of very long chain fatty acids (VLCFAs). A paralogous gene, *gl8b*, has been identified that is 96% identical to *gl8a*. The *gl8a* and *gl8b* genes map to syntenic chromosomal regions, have similar, but not identical, expression patterns, and encode proteins that are 97% identical. Both of these genes are required for the normal accumulation of cuticular waxes on seedling leaves. The chemical composition of the cuticular waxes from *gl8a* and *gl8b* mutants indicates that these genes have at least overlapping, if not redundant, functions in cuticular wax biosynthesis. Although *gl8a* and *gl8b* double mutant kernels have endosperms that cannot be distinguished from wild-type siblings, these kernels are non-viable because their embryos fail to undergo normal development. Double mutant kernels accumulate substantially reduced levels of VLCFAs. VLCFAs are components of a variety of compounds, for example, cuticular waxes, suberin, and sphingolipids. Consistent with their essential nature in yeast, the accumulation of the ceramide moiety of sphingolipids is substantially reduced and their fatty acid composition altered in *gl8a* and *gl8b* double mutant kernels relative to wild-type kernels. Hence, we hypothesize that sphingolipids or other VLCFA-containing compounds are essential for normal embryo development.

Keywords: cuticular waxes, very long chain fatty acids, embryo lethal, sphingolipids.

Introduction

Fatty acids with chain lengths of 20 or more carbons are referred to as very long chain fatty acids (VLCFAs). VLCFAs are components of various lipids whose accumulation is developmentally and spatially regulated. For example, VLCFAs are components of the waxes that cover aerial plant surfaces; of suberin, which accumulates in roots, xylem, and bark, and in response to wounding; and of the sphingolipid portion of plasma membranes. Finally, in seeds of certain species (particularly of the Brassicaceae) VLCFAs are incorporated into triacylglycerol molecules that form the seed oil.

Very long chain fatty acids are biosynthesized by an endoplasmic reticulum (ER)-associated enzyme system, referred to as fatty acid elongase (von Wettstein-Knowles, 1982). Fatty acid elongase generates VLCFAs by elongating 18C fatty acids generated by the plastidic *de novo* fatty acid biosynthetic machinery. The enzymatic mechanism of fatty acid elongation is believed to be analogous to that of

de novo fatty acid synthesis, in that both involve cyclic reactions of ketoacyl synthesis, 3-ketoacyl reduction, 3-hydroxyacyl dehydration, and enoyl reduction (Fehling and Mukherjee, 1991). However, the insoluble nature of the fatty acid elongase system has hampered efforts to purify the system and to identify the genes that encode the component proteins.

In contrast, the characterization of mutants defective in VLCFA biosynthesis (James *et al.*, 1995) or the accumulation of cuticular waxes (Schnable *et al.*, 1994) has resulted in the isolation of three enzyme components of fatty acid elongase. Specifically, characterization of the *fae1* and *cer6* mutants of Arabidopsis resulted in the isolation of genes encoding the ketoacyl-CoA synthase (KCS) (Barret *et al.*, 1998; Fiebig *et al.*, 2000; James *et al.*, 1995; Lassner *et al.*, 1996; Millar *et al.*, 1999; Todd *et al.*, 1999) component of the fatty acid elongase. Similarly, molecular characterization of the maize *gl8* mutant resulted in the identification of the second component of the fatty acid elongase, which catalyzes the 3-ketoacyl reductase (KCR) reaction (Xu *et al.*, 1997, 2002). A gene encoding this enzyme has also been identified in Arabidopsis by DNA sequence similarity (Xu *et al.*, 1997) and subsequently shown to complement a yeast mutant that lacks KCR activity (Beaudoin *et al.*, 2002). More recently, the enoyl reductase component of the fatty acid elongase has also been isolated (Gable *et al.*, 2004; Kohlwein *et al.*, 2001). Genes encoding the remaining component have not yet been identified.

The cuticle is composed of the polymer cutin and a mixture of VLCFA-derived compounds commonly termed cuticular waxes. Some of the cuticular waxes are embedded within the cutin. Others, the epicuticular waxes, are often crystal-like structures visible on the surface of the cuticle. The cuticle of plants limits non-stomatal water loss (Kolattukudy, 1981; Martin and Juniper, 1970) and is thought to provide protection from UV radiation (Reicosky and Hanover, 1978) and various pathogens (Jenks *et al.*, 1994; Kolattukudy, 1987). In addition, the cuticle functions in pollen–stigma (Preuss *et al.*, 1993) and plant–insect interactions (Eigenbrode and Espelie, 1995; Eigenbrode and Shelton, 1990).

Because mutants defective in the normal accumulation of cuticular waxes present a characteristic shiny or glossy appearance, they are readily identifiable (Schnable *et al.*, 1994) and have the potential of providing detailed insights into the function of this protective, lipid-based outer layer of plants. Furthermore, characterization of such mutants provides insights into the biosynthesis of the VLCFA-derived cuticular waxes. Chemical analyses of cuticular waxes isolated from such mutants, in addition to studies of the effects of inhibitors of cuticular wax biosynthesis and radiotracer studies, have been interpreted to indicate that plants contain at least three distinct pathways leading to the biosynthesis of cuticular waxes: the decarbonylation, reduction, and 3-ketoacyl-elongation pathways (reviewed by Post-Beittenmiller, 1996; von Wettstein-Knowles, 1993). The decarbonylation pathway produces alkanes and ketones with odd-numbered carbon chain lengths; the reduction pathway produces alcohols, aldehydes, and esters; and the 3-ketoacyl-elongation pathway produces a variety of oxygenated hydrocarbons. The contribution of each pathway to the final cuticular wax load varies among organs and species.

Although individual biochemical steps required in the biosynthesis of cuticular waxes have been elucidated, the details of the three pathways and their inter-relationships are not well understood. For example, it is not clear whether a single or multiple fatty acid elongases generate the VLCFAs that are the precursors of each pathway. The finding that the Arabidopsis genome contains at least 21 genes that code for KCS (Beisson *et al.*, 2003; Trenkamp *et al.*, 2004) and more than a dozen *KCS* homologs have been identified and mapped in maize (C. R. Dietrich, G.-Y. Wang, B. J. Nikolau and P. S. Schnable, unpublished data) suggests that multiple fatty acid elongases may exist in plants. These results are consistent with the findings that at least three fatty acid elongase-containing preparations with different substrate or co-factor requirements have been partially purified from various membrane extracts (Domergue *et al.*, 1998, 1999; Lessire *et al.*, 1985).

This study reports the isolation and characterization of two paralogous maize genes that encode KCR. These genes have been termed *gl8a* and *gl8b* [the 'original' *gl8* gene cloned by Xu *et al.* (1997) is now referred to as *gl8a*]. A reverse genetic approach was taken to isolate a mutant of *gl8b*. Analyses of *gl8a* and *gl8b* single mutants, and *gl8a*, *gl8b* double mutants establish that the KCR component of fatty acid elongase is essential for normal maize development and that the two genes have at least overlapping, if not identical, functions.

Results

Isolation of a gl8 *paralog*

Based on findings that will be presented in this study, the maize *gl8* locus, which was initially identified by a mutation that caused a reduction in the accumulation of epicuticular waxes on the seedling leaves (Emerson *et al.*, 1935), will henceforward be referred to as *gl8a*. This gene was cloned by identifying a *Mu8* transposon that co-segregated with the glossy phenotype in a stock segregating for the *gl8a-Mu 88-3142* allele (Xu *et al.*, 1997). The sequences of a 6.8-kb *Hin*dIII fragment from the B73 *gl8a* genomic clone λ1512-38 and of an apparently full-length *gl8a* cDNA (pgl8) have been reported previously (GenBank accessions AF302098 and U89509).

RNA gel-blot experiments revealed that seedlings homozygous for *gl8a-ref* or *gl8a-Mu 88-3142* accumulate less *gl8a*-hybridizing mRNA than do normal seedlings (Xu *et al.*, 1997). More recently, RNA gel-blot experiments established

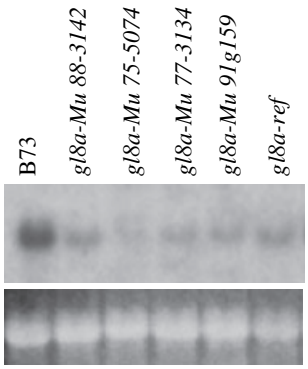

Figure 1. RNA gel-blot analysis of *gl8* transcripts. Each lane contains 15 μg of RNA extracted from the aerial portions of 7-day-old seedlings of the inbred line B73 or homozygous for one of the five indicated *gl8a* mutants. RNA gel-blots were hybridized with a ^{32}P-labeled probe from clone pGAB23. Ethidium bromide-stained 26S rRNAs are shown below.

that multiple *gl8a* alleles that contain *Mu* insertions within their coding regions also accumulate detectable levels of the *gl8a* mRNA (Figure 1). The 1.4-kb *gl8a*-hybridizing mRNA that is detectable in these mutant seedlings may be the consequence of somatic excision events that occur frequently in *Mu* insertion alleles (Doseff *et al.*, 1991). To test the hypothesis that this mRNA is derived from the *gl8a* gene, gel-blot analyses were conducted on RNA isolated from seedlings homozygous for a deletion of the entire *gl8a* locus, *gl8a-Mu 91g159* (Dietrich *et al.*, 2002). As shown in Figure 1, the *gl8a*-hybridizing mRNA is detected in seedlings homozygous for this deletion of the *gl8a* gene. This result demonstrates that the maize genome contains a gene that cross-hybridizes to *gl8a* and that is expressed in seedlings that lack a functional copy of *gl8a*.

This duplicate gene was cloned during the molecular characterization of the *gl8a* gene. Efforts to isolate a *gl8a* cDNA resulted in the isolation of two distinct classes of *gl8a*-hybridizing cDNAs that have nearly identical DNA sequences but that exhibit a few DNA sequence polymorphisms relative to each other and to the *gl8a* genomic clone λ1512-38 (Xu *et al.*, 1997; X. Xu, B. J. Nikolau and P. S. Schnable, Unilever, Bound Brook, NJ, USA, unpublished data). For example, although some *gl8a* cDNA clones (viz., the 0.8-kb partial cDNA clone, p88m, and the 1.4-kb apparently full-length cDNA clone, pgl8) are identical in sequence to the genomic clone λ1512-38, a second class of cDNA clones (viz., the partial 1.0- and 0.5-kb *gl8a*-hybridizing cDNA clones, 1746-10 and 3-1, respectively) contain several single nucleotide polymorphisms (SNPs) and a 10-nt deletion in their 3′-untranslated regions (UTRs) relative to the *gl8a* cDNA and genomic sequences.

The isolation of a *gl8a*-hybridizing B73 genomic clone (λ5-1-1) that exhibited the sequence polymorphisms that distinguish clones 1746-10 and 3-1 from the *gl8a* cDNA clones and the *gl8a* genomic clone established the existence of the *gl8b* gene. Sequence analysis of a 7.2-kb region of clone λ5-1-1 (GenBank accession AF527771) revealed that the *gl8a* and *gl8b* genes have conserved gene structures including absolute conservation of their intron/exon borders (Figure 2). The differences in the sequences of the two genes are largely a consequence of the presence of SNPs and small insertion/deletion polymorphisms (IDPs) ranging in size from one to 35 nt. The protein-coding regions exhibit 96% nucleotide identity while their introns exhibit approximately 85% nucleotide identity. The 3′-UTRs are 92% identical with a 10-nt IDP accounting for the largest difference. In contrast, significant differences exist between the 5′-UTRs and the non-transcribed regions of the two genes. Based on the apparently full-length *gl8a* cDNA (Xu *et al.*, 1997), the 5′-UTR of *gl8a* is at least 130 nt in length. In contrast, 5′-RACE experiments indicate that the 5′-UTR of *gl8b* is only between 30 and 36 nt in length. Excluding the four nt immediately 5′ of the start codon, no regions of sequence identity are

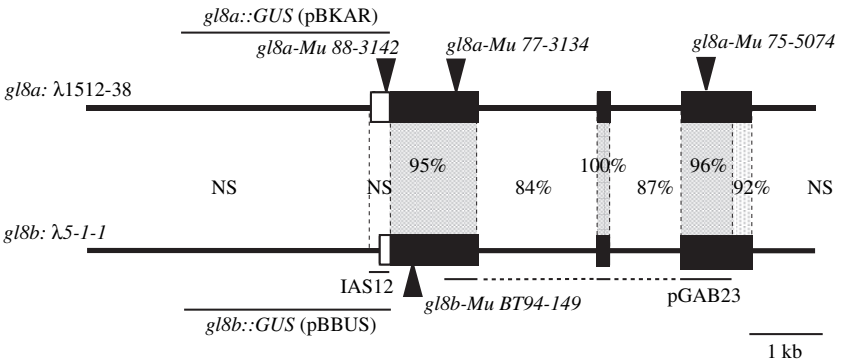

Figure 2. Structures of the *gl8a* and *gl8b* genes. The percentage sequence identity is indicated for each region of the *gl8a* (clone λ1512-38) and *gl8b* (clone λ5-1-1) genes. NS, no regions of identity according to the BESTFIT algorithm in the GCG software package (version 10.0-Unix, from the Genetics Computer Group, Madison, WI, USA) with a gap creation penalty of 50 and a gap extension penalty of 3. *Mu* transposon insertion sites for alleles *gl8a-Mu 88-3142*, *gl8a-Mu 77-3134*, *gl8a-Mu 75-5074*, and *gl8b-Mu BT94-149* sites are indicated by triangles. Regions used in the promoter::GUS fusion constructs *gl8a::GUS* (pBKAR) and *gl8b::GUS* (pBBUS), the *gl8b*-specific probe IAS12, and pGAB23 are indicated. pGAB23 is derived via PCR amplification of the *gl8a* cDNA (pgl8) and thus contains only those regions indicated by the solid line.

detected in GCG BESTFIT or DOTPLOT alignments between the regions of *gl8a* and *gl8b* 5′ of their start codons. Sequence identity also deteriorates rapidly downstream of the 3′-UTRs of these paralogs.

A region of the genomic clone λ5-1-1 specific to the *gl8b* gene (probe IAS12, Figure 2) was PCR amplified and used as a restriction fragment length polymorphism (RFLP) probe in DNA gel-blot experiments. Hybridization to the recombinant inbreds developed by Burr and Burr (1991) established that *gl8b* maps to chromosome 4L, 0.6 cM from RFLP marker bnl7.20. In contrast, the *gl8a* gene maps to chromosome 5L tightly linked (<1 cM) to the *pr* gene (Coe, 1993; Stinard and Schnable, 1993). Chromosomes 4L and 5L are syntenic (Devos and Gale, 1997) suggesting that *gl8a* and *gl8b* are paralogs.

gl8-*encoded proteins*

The *gl8a* and *gl8b* genes are both predicted to encode 326 amino acid proteins that are 97% identical with only 11 amino acid differences. Both proteins exhibit sequence similarity to a large class of keto-reductases (Xu *et al*., 1997) that have a signature pattern of conserved Tyr and Lys residues that are thought to be important for catalytic activity (Ensor and Tai, 1991). N-terminal signal peptides with predicted cleavage sites on the carboxyl side of positions 34 and 32 for GL8A and GL8B, respectively, were detected by SignalP (Nielsen *et al*., 1997). Both proteins are predicted by PSORT (Nakai and Kanehisa, 1992) to have a single transmembrane domain spanning residues 71–87 and a cytoplasmic C-terminus. PSORT and TargetP (Emanuelsson *et al*., 2000) predict these proteins are localized to the secretory pathway. The Lys residues at positions −3, −4, and −5 from the carboxyl terminus suggest that GL8A and GL8B are ER proteins (Andersson *et al*., 1999; Jackson *et al*., 1990). Indeed, subcellular localization experiments using polyclonal antibodies raised against the C-terminal 76 amino acids of a recombinant GL8A protein have confirmed that these proteins are localized to the ER (Xu *et al*., 2002). The biochemical function of GL8 as the KCR component of the acyl-CoA elongase was experimentally demonstrated by immuno-inhibition studies (Xu *et al*., 2002).

Isolation of a gl8b *mutant*

As discussed above, RNA-gel blot analyses indicate that *gl8b* mRNA accumulates to detectable levels in both normal and *gl8a* mutant seedlings (Figure 1). In addition, Western analyses conducted with polyclonal antibodies raised against recombinant GL8A detect this protein in microsomal extracts from seedlings homozygous for a *gl8a* mutant (data not shown). These data, in conjunction with the glossy phenotype associated with *gl8a* mutations, indicate that *gl8b* cannot substitute for *gl8a* mutations in epicuticular wax biosynthesis even though the GL8B protein accumulates in seedling leaves and is 97% identical to GL8A.

To determine the role of *gl8b* a reverse genetic approach was used to identify a mutant allele of this gene. The Trait Utility System for Corn (TUSC) (Bensen *et al*., 1995) was used to screen a large population of plants generated from active *Mu* stocks to identify individuals that carried a *Mu* insertion in the *gl8b* gene. A *Mu* insertion allele, *gl8b-Mu BT94-149*, was identified via this approach, and sequence analyses established that it contains a *Mu1* insertion 140 bp downstream of the start codon in exon 1 (GenBank accession AF527772, Figure 2).

F_2 progeny carrying *gl8b-Mu BT94-149* segregated 3:1 for lethal virescent seedlings. Genotyping of these F_2 seedlings established that the virescent phenotype was due to an independent mutation in coupling with *gl8b-Mu BT94-149* and located approximately 15 cM from *gl8b*. Plants homozygous for *gl8b-Mu BT94-149* that carry at least one chromosome in which a crossover occurred between the virescent mutant and the *gl8b* locus do not have any obvious mutant phenotype at the seedling stage, viz., they are not glossy. In fact, it has not been possible to identify any visible morphological phenotype at any stage in plant development that is associated with homozygosity for *gl8b-Mu BT94-149*. However, scanning electron microscopy (SEM) images of seedlings homozygous for the *gl8b* mutant from an F_2 stock that is not segregating for the virescent mutation reveal either no difference or only a slight decrease in the number of epicuticular wax crystals relative to wild-type siblings from the same F_2 family (Figure 3). In contrast, SEMs of a seedling leaf at a similar stage from a plant homozygous for the *gl8a-Mu 88-3142* allele reveal the surface is nearly devoid of epicuticular wax crystals (Figure 3).

Chemical analysis of cuticular waxes

The chemical composition of the cuticular waxes from leaves of seedlings of the wild-type inbred B73, and seedlings homozygous for *gl8b-Mu BT94-149* or *gl8a-Mu 77-3134* were determined by GC-MS. The major components of the cuticular wax of wild-type (B73) seedling leaves are C32 fatty acid derivatives, namely C32 alcohols and C32 aldehydes, which together account for about 91% of the wax (Figure 4; Tables S1 and S2). The difference between this composition and that reported previously (Bianchi *et al*., 1979, 1985) is primarily in the ester fraction, which accounts for <1% of the wax in our studies (Figure 4; Tables S1 and S2), but 15% of the wax from the inbred Wf9. We have confirmed that this difference is due to the different genetic backgrounds used in these two studies (M. A. D. N. Perera, P. S. Schnable and B. J. Nikolau, unpublished data).

Seedlings homozygous for *gl8a* or *gl8b* mutants accumulate cuticular waxes to levels of only 5 and 50% of those that accumulate on wild-type seedlings, respectively (Figure 4a).

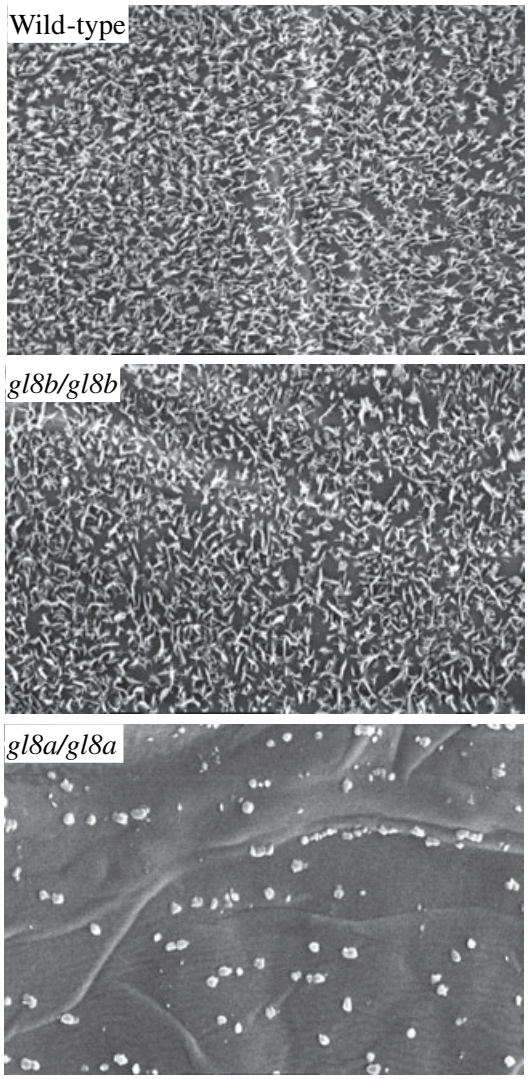

Figure 3. Effects of *gl8a* and *gl8b* mutations on epicuticular wax deposition. SEM images at 5000× magnification from the adaxial surface of the second leaves from 10-day-old seedlings. Images are from a wild-type plant, a plant homozygous for *gl8b-Mu BT94-149*, and a plant homozygous for *gl8a-Mu 88-3142*.

When compared with the wild-type control, the inbred B73, the carbon chain lengths of the cuticular wax components are significantly shorter in *gl8a* mutants, but are less affected in *gl8b* mutants (Figure 4d; Table S3). In the wild type, 31- and 32-carbon components account for more than 95% of the cuticular waxes. These 'fully' elongated components account for 83% of the cuticular waxes of the *gl8b* mutant. In contrast, in the *gl8a* mutant, only 35% of the cuticular wax components are derivatives of fully elongated fatty acids. Interestingly, in this mutant, but not *gl8b*, non-elongated (i.e., 12–18 carbons) fatty acid derivatives account for nearly 20% of the cuticular wax components.

In all three genotypes the predominant components are free alcohols and aldehydes. With the exception of esters

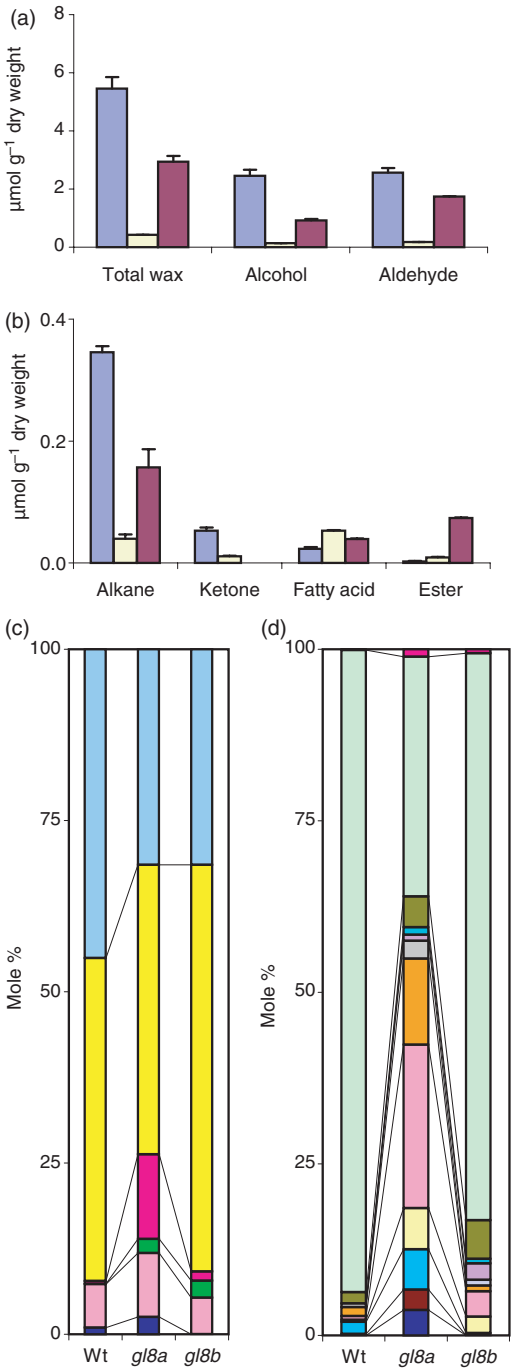

Figure 4. Composition of the cuticular waxes of seeding leaves.
(a, b) Cuticular waxes were extracted and analyzed from wild type (□), *gl8b-Mu BT94-149* (■) and *gl8a-Mu 77-3134* (□) seedling leaves as described in the Experimental procedures. Analyses were conducted in triplicate and the average (± standard deviation) is shown.
(c) The effect of the *gl8a* and *gl8b* mutations on the mole proportion of the cuticular wax components: alcohols (□), aldehydes (□), alkanes (□), methylketones (■), fatty acids (■), and esters (■).
(d) The effect of the *gl8a* and *gl8b* mutations on the carbon chain lengths of all cuticular wax components: $C_{11} + C_{12}$ (■), $C_{13} + C_{14}$ (■), $C_{15} + C_{16}$ (■), $C_{17} + C_{18}$ (□), $C_{19} + C_{20}$ (□), $C_{21} + C_{22}$ (■), $C_{23} + C_{24}$ (□), $C_{25} + C_{26}$ (□), $C_{27} + C_{28}$ (■), $C_{29} + C_{30}$ (■), $C_{31} + C_{32}$ (□), and $C_{33} + C_{34}$ (■).

and free fatty acids, the chemical composition of the cuticular waxes on the *gl8a* and *gl8b* mutants, on a percentage basis, is not dramatically different than those of wild-type seedlings (Figure 4c; Table S1).

Alcohols and alkanes are both derived from aldehydes. In the wild type the chain length distributions of the aldehyde and alcohol fractions are similar to each other but differ from that of the alkanes (Figures S1–S3). Aldehydes and alcohols consist primarily of 32 carbons, whereas a large proportion (i.e., approximately 60%) of the alkanes contain 29 or fewer carbons. Although the distribution of the chain lengths of free alcohols and aldehydes differs between the *gl8a* and *gl8b* mutants, each mutant similarly affects the chain length distribution of these two cuticular wax components, in that shorter molecules accumulate in both mutants (compare Figures S1 and S2). Interestingly, the *gl8a* and *gl8b* mutations have a less dramatic impact on the chain length distribution of alkanes (Figure S3).

Here, we report the identification of ketones in the cuticular waxes of maize seedling leaves; these are methyl ketones, with the carbonyl group situated on the second carbon atom of the molecule. These molecules account for only a small proportion of the cuticular waxes of wild-type seedlings (1%, Figure 4b,c). The accumulation of ketones is dramatically reduced in the *gl8a* mutant and completely eliminated in the *gl8b* mutant. The carbon chain length of those ketones that do accumulate in the *gl8a* mutant is shorter than in the wild-type control (Figure S4; Table S1).

When compared with wild type, more esters accumulate in the *gl8* mutants and this effect is especially pronounced in the *gl8b* mutant (Figure 4b,c; Table S2). Both *gl8* mutations also cause compositional changes in the ester fraction (Figure S6; Table S2). Whereas esters of wild-type seedlings are predominantly of 52 carbons (C-22 acid esterified to C-30 alcohol and C-20 acid esterified to C-32 alcohol), in both *gl8* mutants these C-52 esters are undetectable but are replaced by shorter esters of between C36 and C48. This shortening of the ester chain length is more pronounced in *gl8b* than in *gl8a* (Figure S6; Table S2). Shortening of the carbon chains is primarily due to shortening of the esterified alcohol moiety. In fact, the effect of *gl8* mutations on the chain length of esterified alcohol moieties reflects the reduction in the chain length distribution of the free alcohol pool. In contrast, there is no direct relationship between the carbon chain length distribution of the free and esterified acid fractions (compare Figures S5 and S6). This is apparent in all three genotypes, even though the accumulation of free fatty acids is increased in one of the mutants, that is, the *gl8a* mutant (Figure 4b,c).

Expression patterns of gl8a *and* gl8b

The high level of sequence identity in the coding regions of *gl8a* and *gl8b* and the small size of the *gl8b* 5′-UTR make it difficult to design probes that can distinguish between the transcripts from these two genes. This challenge was overcome by making use of the fact that RNA samples from *gl8a* mutant plants contain only *gl8b* mRNA and RNA samples from *gl8b* mutant plants contain only *gl8a* mRNA. Thus, it was possible to monitor the expression patterns of these genes individually via RNA gel-blot analyses performed with RNA isolated from plants that were homozygous for the *gl8a* or *gl8b* mutations. Hybridization was performed with a probe generated from a portion of the *gl8a* cDNA (clone pGAB23, Figure 2) that detects both *gl8a* and *gl8b* mRNAs.

RNA gel-blot analyses detect an approximately 1.4-kb *gl8*-hybridizing mRNA in all samples from *gl8a* and *gl8b* mutant plants as well as from wild-type plants (Figure 5a–c). The *gl8b* mRNA accumulates at its highest levels in husk, tassel, and young ears. The *gl8a* mRNA accumulates to its highest levels in seedlings, silk, and young ears. In most samples, the *gl8a* mRNA accumulates to approximately 5- to 10-fold higher levels than the *gl8b* mRNA. Wild-type plants accumulate *gl8*-hybridizing mRNA to levels that are approximately equal to the sum of the *gl8a* and *gl8b* mRNAs detected in the mutant plants (compare Figure 5a with 5b,c). Hence, it appears that the expression of the *gl8a* gene is not affected by the absence of a functional copy of *gl8b* or that the expression of the *gl8b* gene is not affected by the absence of a functional copy of *gl8a*.

To better localize the *gl8*-hybridizing mRNAs in seedlings, the above ground portion of 10-day-old B73 seedlings was divided into expanded and unexpanded portions. The expanded sample contained only the leaf blades of the fully expanded first and second leaf while the unexpanded sample consisted of the sheaths of leaves 1 and 2 and the unexpanded leaves encircled by those sheaths. The *gl8* mRNAs were detected almost exclusively in the RNA from the unexpanded leaf sample (Figure 5d).

Transgenic analysis

To further aid in the characterization of the expression of these paralogs, we developed transgenic maize lines carrying the GUS reporter, regulated by the promoters from either the *gl8a* or the *gl8b* gene. Approximately 2-kb fragments of DNA upstream of the *gl8a* and *gl8b* start codons were transcriptionally fused to the GUS gene in the pDMC205-vector to generate *gl8a::GUS* and *gl8b::GUS* transgenes, respectively.

Fourteen independent transgenic lines were generated that carry *gl8a::GUS*, five of which expressed GUS over multiple generations. In seedling leaves, the expression of *gl8a* is highest in the innermost young leaves still enclosed within the coleoptile (Figure 6a); interestingly, *gl8a* is not expressed to detectable levels in the coleoptile. Moreover, in these inner leaves *gl8a* expression is not cell specific. In

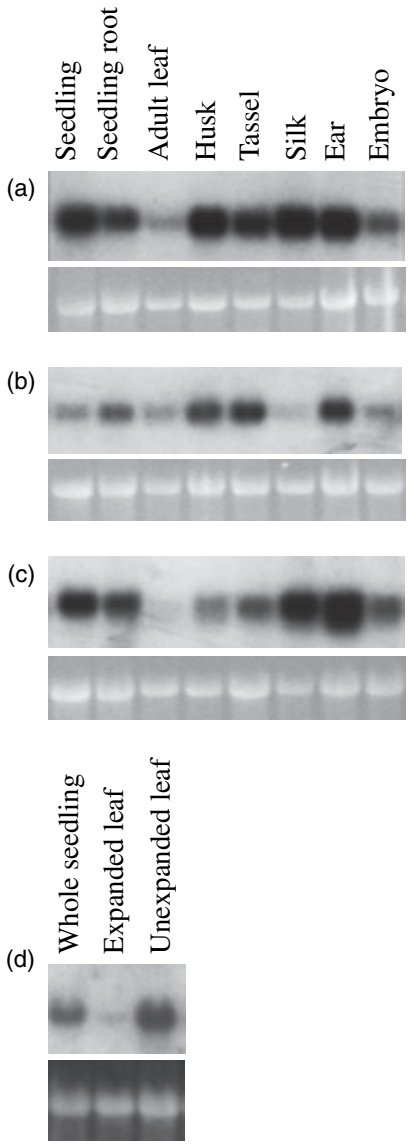

Figure 5. Accumulation of *gl8a* and *gl8b* mRNAs in various maize organs. Each lane contains approximately 10 μg of RNA. RNA gel blots were hybridized with a ^{32}P-labeled probe from clone pGAB23.
(a) The hybridization signal detected in B73 measures the accumulation of both the *gl8a* and *gl8b* mRNAs.
(b) The hybridization signal detected in *gl8a-Mu 91g159* homozygotes measures the accumulation of *gl8b* mRNA.
(c) The hybridization signal detected in *gl8b-Mu BT94-149* homozygotes measures the accumulation of *gl8a* mRNA.
(d) Aerial portions of 10-day-old B73 seedlings separated into expanded and unexpanded leaf samples. Ethidium bromide-stained 26S rRNAs are shown below each RNA gel blot.

contrast, in the unexpanded portion of the outermost true leaf, *gl8a* expression is restricted to the epidermal cells and vascular bundles. Furthermore, in the expanded portion of this leaf, *gl8a* expression is maintained only in the vascular bundles, that is, expression is lost in epidermal cells (data not shown). These findings are consistent with the RNA gel blots shown in Figure 5(d), which demonstrated that *gl8* expression is highest in unexpanded portions of seedling leaves. Similarly, in adult leaves, GUS expression is detected only in the vascular tissue (data not shown). GUS activity is also observed in seedling roots, with the most intense staining near the root tips and positions in the root nearest the pericycle where lateral roots emerge; weak staining is also apparent in the vascular tissue (Figure 6b).

Cross sections of young pistillate spikelets and cob reveal GUS staining in the pith and in a small region within the ovule that appears to be the nucellus (data not shown). In mature unpollinated ears, GUS activity is most obvious at the base of the silk where cell division occurs (Figure 6c). A heavily stained spot is often observed at the base of the silk (Figure 6c, arrow). This spot represents the tip of the posterior carpel that marks the location of the stylar canal (Kiesselbach, 1949). GUS activity is minimal through much of the remainder of the silk, although it is often observed in silk hairs (data not shown). In staminate flowers, expression is not only most prominent in pollen grains (Figure 6d), but is also observed in the vascular tissue of glumes (data not shown). GUS staining is observed first in pollen grains near

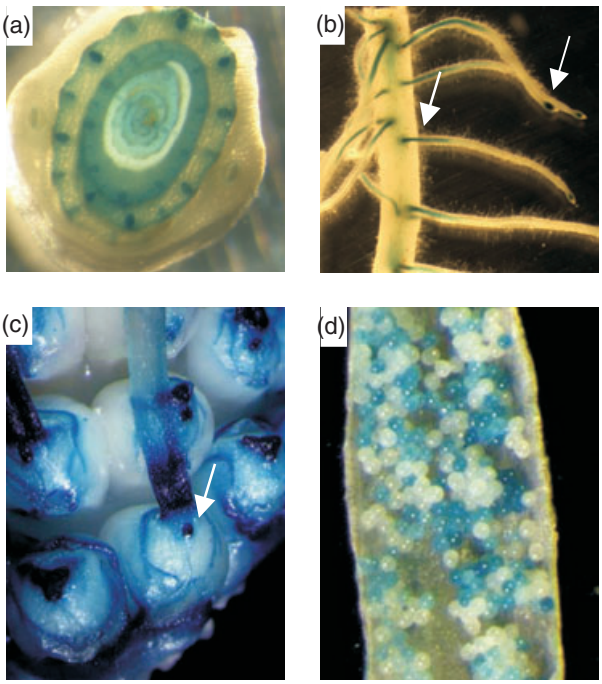

Figure 6. Histochemical staining of *gl8a::GUS* expression. All images are from plants hemizygous for the *gl8a::GUS* transgene.
(a) Cross section through coleoptile and inner leaf from a 7-day-old seedling.
(b) Portion of the primary root from a 7-day-old seedling. Arrows indicate regions of high GUS activity in the root meristem and portion of the root nearest the pericycle.
(c) Base of silk from mature unpollinated ear. The spot indicated by the arrow is the tip of the posterior carpel.
(d) Dissected anther containing pollen segregating 1:1 for the transgene. GUS staining patterns for the *gl8b::GUS* transgene are indistinguishable from the staining patterns obtained from *gl8a::GUS*.

the tip of the anther but over the few days prior to anthesis pollen grains lower in the anther begin to stain.

In parallel, 11 independent transgenic lines were generated that carry *gl8b::GUS*, four of which expressed GUS over multiple generations. Although some variation was observed in the levels of expression among *gl8a::GUS* and *gl8b::GUS* events, overall and throughout development, the patterns of *gl8b*-driven GUS expression are indistinguishable from those of *gl8a*-driven GUS expression (data not shown). Because both strongly and weakly expressing events were recovered for each transgene, this variation in the level of GUS activity likely reflects variation arising from transgene position effects rather than differences in promoter activities.

The experiments described above were conducted in a stock that carried functional alleles of *gl8a* and *gl8b*. The patterns of *gl8a* and *gl8b*-driven GUS expression were also assayed in stocks that were homozygous for the *gl8a-ref* mutation. No differences in the levels or the patterns of expression were observed for either the *gl8a::GUS* or *gl8b::GUS* transgene in the *gl8a-ref* mutant background (data not shown). This indicates that expression of *gl8a* and *gl8b* is not affected by the absence of a functional copy of *gl8a*, a result that is consistent with RNA gel-blot analyses (Figure 5) that suggest that the accumulation of *gl8b* mRNA is not influenced by the absence of a functional copy of *gl8a*.

In situ *hybridization*

In situ hybridization was used to confirm many of the expression patterns obtained by observing GUS staining patterns in transgenic plants. Digoxigenin-labeled antisense and sense RNA probes were generated from the same *gl8a* cDNA clone (pGAB23) from which a probe was generated for the RNA gel-blot experiments. Thus, as with the gel-blot analyses (Figure 5), the *gl8b* mRNA is specifically detected in *gl8a* mutants, the *gl8a* mRNA is specifically detected in *gl8b* mutants and both mRNAs are detected in wild-type plants.

Consistent with RNA gel-blots and analyses of transgenic plants, *in situ* hybridizations to cross sections of the young unexpanded portions of 7-day-old seedlings from B73, and *gl8a* and *gl8b* mutants revealed that the highest level of *gl8* mRNA accumulation occurs in the innermost leaves, where accumulation is fairly homogeneously distributed among cell types. In outer leaves, however, *gl8* mRNA accumulation is restricted to the vascular tissue and epidermal cells (Figure 7a–f). Consistent with the analysis of the *gl8::GUS* transgenic plants, only limited accumulation of *gl8* mRNAs is observed in the coleoptile. The spatial patterns of mRNA accumulation appear similar for *gl8a* and *gl8b*, although, consistent with RNA gel-blot experiments, the accumulation of *gl8a* mRNA is considerably higher than that of *gl8b*.

In situ hybridizations of longitudinal sections through a B73 kernel imbibed for 48 h revealed that the *gl8* mRNAs accumulate in the vascular tissue of the scutellum and throughout the embryo axis (Figure 7g,j). *gl8* mRNAs accumulate throughout the root but to highest levels in the endodermis (Figure 7h,k). *In situ* hybridizations of longitudinal sections through a wild-type (inbred line Ky21) ear revealed high levels of *gl8* mRNAs throughout this organ, with the highest levels accumulating in the developing ovules (Figure 7i,l). Consistent with the low level of *gl8* expression in adult leaves, as revealed by RNA gel-blot and transgenic analyses, *in situ* hybridizations failed to detect *gl8* mRNAs in these organs (data not shown).

gl8a, gl8b *double mutants*

The overlapping expression pattern of the *gl8* paralogs, in addition to the very similar composition of the waxes that form on mutants of these two genes, led us to hypothesize that the *gl8a* and *gl8b* genes have at least partially redundant functions. To test this hypothesis double mutants were generated. Crosses were made between stocks homozygous for *gl8a-Mu 88-3142* and *gl8b-Mu 94BT-149* (cross 1). One copy of chromosome 4 in the stock homozygous for *gl8b-Mu 94BT-149* also carried the linked *v** mutation, which confers a recessive virescent phenotype. F_1 plants from this cross were self-pollinated and F_2 progeny scored for *gl8a*, *gl8b* double mutants. Because *gl8a* and *v** are unlinked, F_2 progeny from F_1 plants that inherited the *gl8b-Mu 94BT-149 v** chromosome (cross 2) were expected to segregate 3:1 for glossy (because of homozygosity for *gl8a*); further, because *gl8a* and *gl8b* are unlinked, one-quarter of these glossy seedlings were expected to be virescent (because of homozygosity for *v**). However, glossy, virescent seedlings were observed at a rate substantially lower than expected. In fact, only 13 of 165 glossy seedlings were virescent. Genotyping of these 13 seedlings revealed that each was heterozygous at the *gl8b* locus, and, therefore, arose via crossovers between *gl8b-Mu BT94-149* and *v**. Hence, no viable *gl8a*, *gl8b* double mutants were recovered out of a population of over 600 F_2 progeny. In addition, genotyping of 300 F_2 progeny from cross 3 (that did not include the *v** marker) also failed to identify double mutant seedlings, although all other possible genotypes were present at ratios expected from a standard di-hybrid cross. This provides strong evidence that the *gl8a*, *gl8b* double mutant genotype is lethal.

Cross 1: *gl8a-Mu 88-3142*/*gl8a-Mu 88-3142*; *Gl8b V**/*Gl8b V** X *Gl8a*/*Gl8a*; *gl8b-Mu BT94-149 v**/*gl8b-Mu BT94-149 V**

Cross 2: *gl8a-Mu 88-3142*/*Gl8a*; *gl8b-Mu BT94-149 v**/*Gl8b V** self

Cross 3: *gl8a-Mu 88-3142*/*Gl8a*; *gl8b-Mu BT94-149 V**/*Gl8b V** self

To distinguish between a double mutant genotype that produces a non-viable kernel or one that is gametophytic

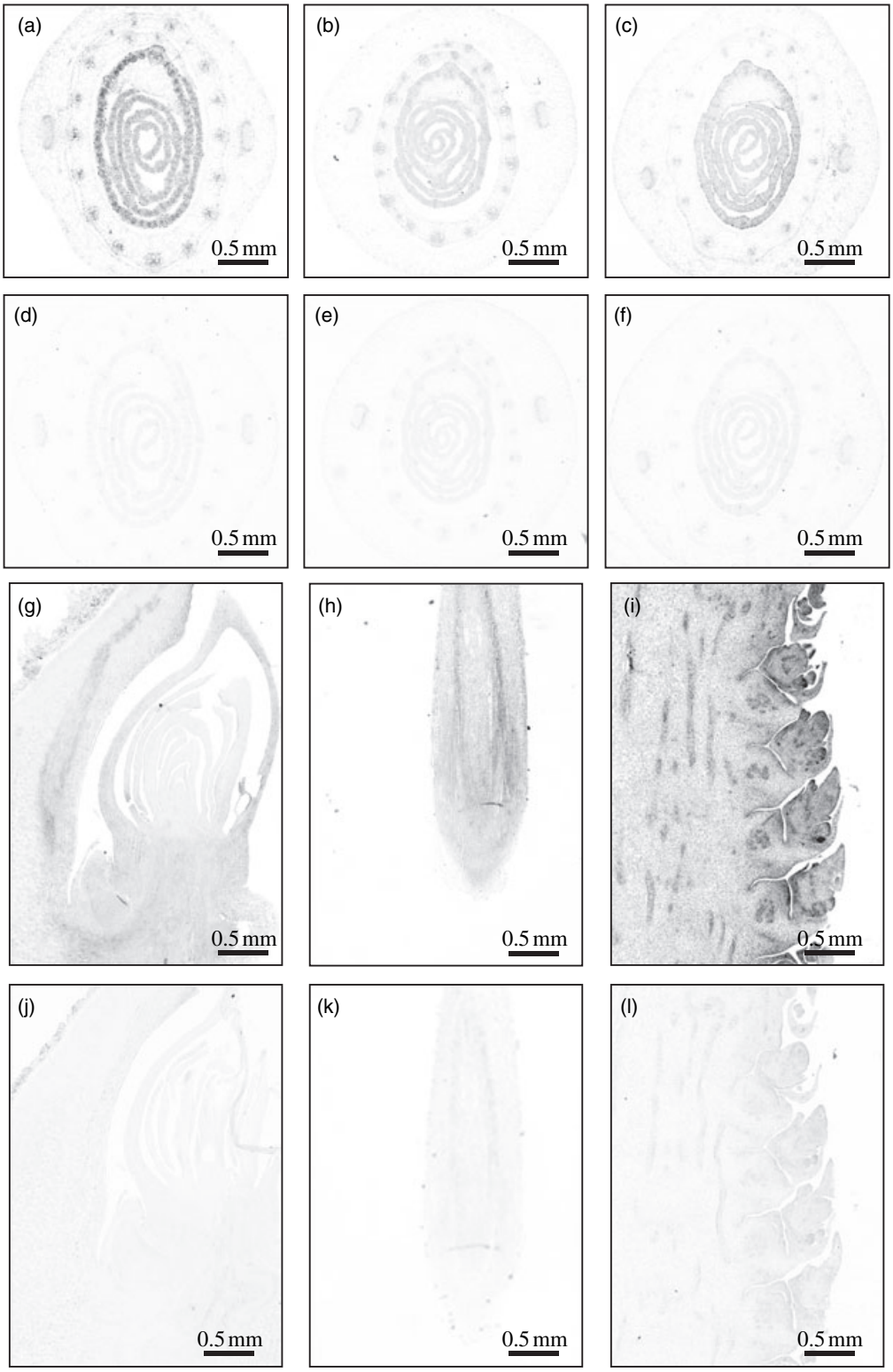

Figure 7. Tissue distribution of *gl8a* and *gl8b* mRNAs. Histological sections were hybridized with probes consisting of either antisense RNA (a–c, g–i) or control sense RNA (d–f, j–l) from the *gl8a* cDNA clone pGAB23. Cross section through coleoptile and inner leaves of 7-day-old seedling from B73 (a, d), homozygous for *gl8a-Mu 91g159* in which only *gl8b* mRNA accumulates (b, e), and *gl8b-Mu BT94-149* in which only *gl8a* mRNA accumulates (c, f). Longitudinal section through embryo axis of a B73 kernel following 48 h of imbibition (g, j). Cross section through primary root tip from B73 48 h after imbibition (h, k). Longitudinal section through immature ear and pistillate spikelets from a non-mutant Ky21 plant (i, l).

lethal, kernels that were expected to segregate 25% for double mutants were germinated in paper rolls (Wen and Schnable, 1994). Approximately 25% of the F_2 kernels from crosses 4 or 5 did not produce viable seedlings (Figure 8a). These non-viable kernels had normal endosperms but degenerated scutella and embryos (Figure 8b). DNA isolated from endosperms of such kernels confirmed that these kernels are double mutant for the *gl8a* and *gl8b* mutations. A small percentage (approximately 5%) of these kernels produce a small primary root without any shoot growth (data not shown). Genotyping of such seedlings (using DNA isolated from roots) revealed that these abnormal seedlings were also homozygous for both *gl8a-Mu 88-3142* and *gl8b-Mu BT94-149*. In very rare instances, limited shoot growth was observed in double mutants but within 24 h of emergence these shoots completely desiccated (data not shown).

Cross 4: *gl8a-Mu 88-3142*/*Gl8a*; *gl8b-Mu BT94-149 V**/*gl8b-Mu BT-149 V**self

Cross 5: *gl8a-Mu 88-3142*/*gl8a-Mu 88-3142*; *gl8b-Mu BT94-149 V**/*Gl8b V** self

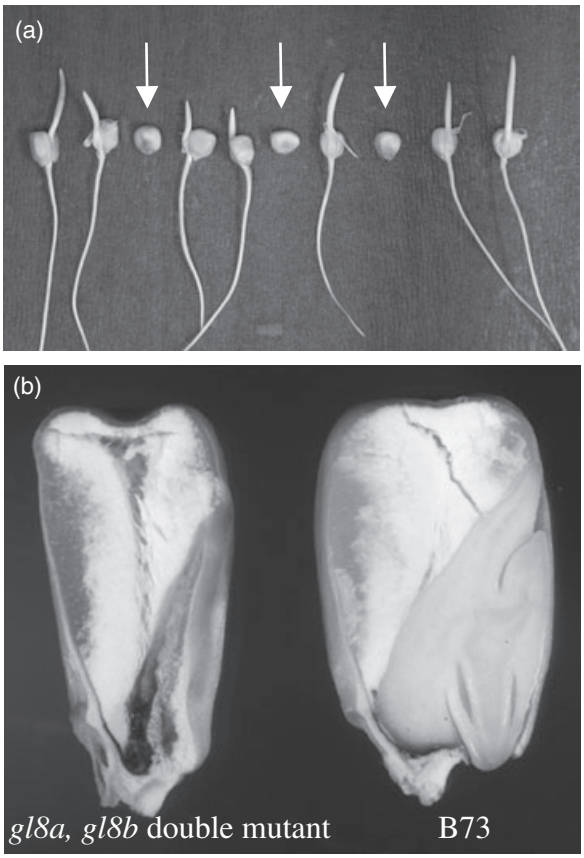

Figure 8. Phenotypes of *gl8a, gl8b* double mutants.
(a) F_2 family from cross 5 in which one-fourths of the 5-day-old seedlings are *gl8a, gl8b* double mutants (arrowed kernels).
(b) Sections of kernels from *gl8a, gl8b* double mutants (left) and non-mutant (B73) (right) following 24 h imbibition.

Chemical analysis of gl8 *mutant kernels*

To understand the biochemical basis of the lethality associated with the *gl8a, gl8b* double mutant, the fatty acids that accumulate in mature kernels were quantified. To analyze total fatty acids, lipids are typically extracted (Bligh and Dyer, 1959) and the associated fatty acids are either saponified and derivatized or directly derivatized. The resulting derivatives, typically methyl esters, are analyzed via GC-MS. This method recovers free fatty acids as well as those that are bound to compounds via ester or thioester bonds. But because this method fails to recover fatty acids that are bound to compounds via amide bonds (e.g., sphingolipids and *N*-acylethanolamides) or fatty acids that have been incorporated into polymers (e.g., cutin or suberin), it underestimates the total fatty acid content of the tissue. Plant tissues were therefore first treated with a strong acid which hydrolyzes all fatty acid-containing compounds, including those bound to amides and polymers. The released free fatty acids were then recovered, methylated, and analyzed via GC-MS. Because the pericarp of kernels consists of maternal tissue (which in some experiments had a genotype that differed from that of progeny tissue of the kernel, that is, the endosperm, aleurone, and embryo), pericarps were removed from all kernels prior to analysis.

The yield of fatty acids from mature wild-type kernels after acid hydrolysis was 60 μmol g^{-1}, when compared with 31 μmol g^{-1} from the saponification of isolated lipids (data not shown). Both methods recovered VLCFAs from kernels (i.e., 20:0, 20:1, 20:2, 22:0, 24:0, and 26:0). However, VLCFAs account for a larger proportion of the fatty acids recovered after acid hydrolysis than via initial lipid extraction (10 and 7% for seeds; Figure S7). This probably reflects the recovery of VLCFAs from sphingolipids and/or suberin, which are not recovered via initial lipid extraction.

Using the acid hydrolysis protocol the accumulation of fatty acids in mature kernels of the *gl8a* and *gl8b* single mutants and the double mutant were compared with the accumulation in wild-type kernels. Wild-type kernels accumulate approximately 4 μmol VLCFAs g^{-1} dry weight (Figure 9a). In contrast, kernels homozygous for the *gl8a* or *gl8b* mutants accumulate 0.55 and 2.9 μmol VLCFAs g^{-1}, respectively. The relative proportions of the 20:0, 20:1, 20:2, 22:0, 24:0, and 26:0 VLCFAs were unaffected by either the *gl8a* or *gl8b* mutant (Figure S7; Table S4). Surprisingly, the *gl8a* mutant (but not *gl8b*) also affects the accumulation of C16 and C18 fatty acids (Figure 9a). Although wild type and *gl8b* mutant kernels each accumulate over 55 μmol C16 and C18 fatty acids g^{-1} dry weight, *gl8a* mutant kernels accumulate only 33 μmol of C16 and C18 fatty acids g^{-1}. The relative proportion of 16:0,18:0, 18:1, and 18:2 was unaffected by the *gl8a* or *gl8b* mutants (Figure S7; Table S4). Reductions in the accumulation of VLCFAs in the *gl8a* and *gl8b* single mutations are consistent with the roles of the GL8A and

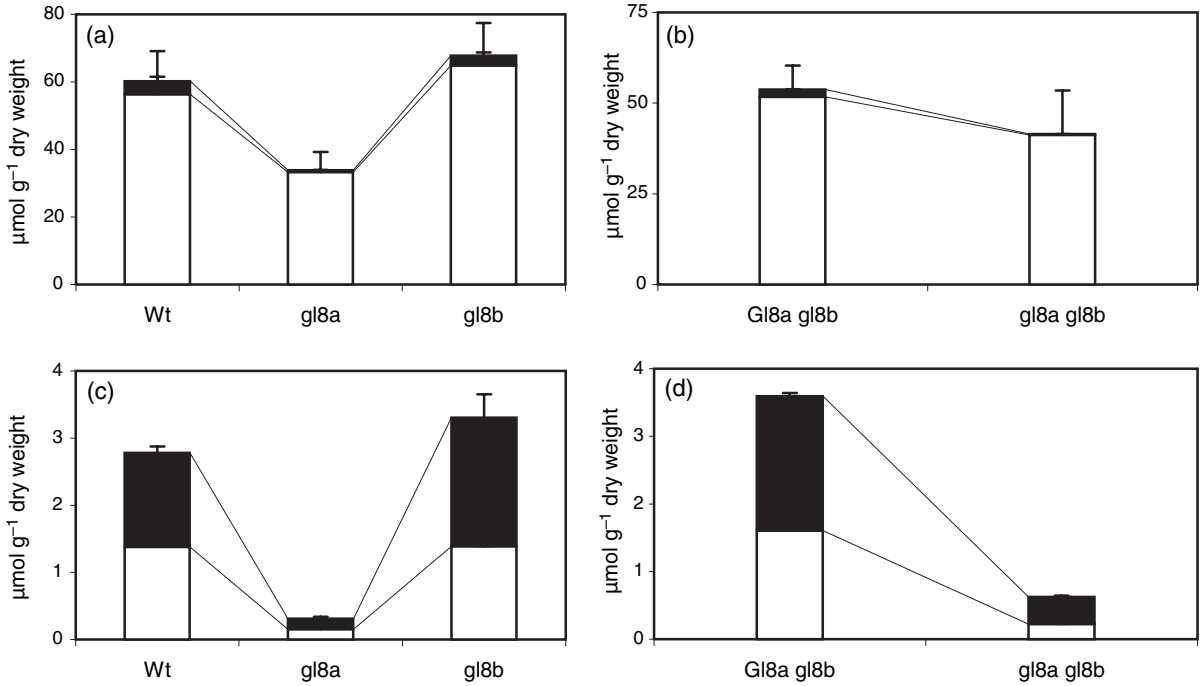

Figure 9. Effects of the *gl8a* and *gl8b* single mutations and the *gl8a*, *gl8b* double mutation on the accumulation of kernel fatty acids and ceramides. C16 and C18 fatty acids (non-shaded area) and VLCFA (black shaded area) are indicated. The statistical significance of differences in the composition of the genotypes was tested with two-tailed Student's *t*-tests. Due to the differences in genetic backgrounds it was only appropriate to conduct these comparisons within individual panels.
(a, b) Total fatty acids were extracted and analyzed from the indicated genotypes as described in Experimental procedures. In (a), the accumulation of VLCFAs in the *gl8a* single mutant is significantly lower than in wild type, but this is not true for the *gl8b* single mutant. In (b), the accumulation of VLCFAs in the *gl8a, gl8b* double mutant is significantly lower than in the *gl8b* single mutant.
(c, d) Ceramides were extracted and analyzed from kernels of the indicated genotypes as described in Experimental procedures. In (c), the accumulation of ceramide-associated fatty acids in the *gl8a* single mutant, but not in the *gl8b* single mutant, is significantly lower than in wild type. In (d), the accumulation of ceramide-associated fatty acids in the double mutant is significantly lower than that in the *gl8b* single mutant.
All analyses were conducted in triplicate and the average (± standard deviation) is shown. Genotypes: wild type (Wt); *gl8a-Mu 77-3134*/*gl8a-Mu 77-3134* (gl8a); *gl8b-Mu BT94-149*/*gl8b-Mu BT94-149* (gl8b); *Gl8a*/*gl8a-Mu 77-3134 gl8b-Mu BT94-149*/*gl8b-Mu BT94-149* (Gl8a gl8b); and *gl8a-Mu 77-3134*/*gl8a-Mu 77-3134 gl8b-Mu BT94-149*/*gl8b-Mu BT94-149* (gl8a gl8b). The two genotypes in (b) and (d) are siblings.

GL8B proteins in the elongation of C18 fatty acids to VLCFAs (Bianchi *et al.*, 1985; von Wettstein-Knowles, 1987; Xu *et al.*, 2002). Moreover, the effect of the *gl8a* mutation is quantitatively more extreme than that of the *gl8b* mutation, a result that is consistent with the fact that the *gl8a* mRNA accumulates to higher levels than the *gl8b* mRNA in the tissues.

Very long chain fatty acids are components of several classes of molecules, including cuticular waxes, suberin, sphingolipids, and some membrane phospholipids and seed oils. Although comprehensive analyses have not yet been conducted, of these VLCFA derivatives, only sphingolipids have been shown to be essential in any biological system (reviewed by Dunn *et al.*, 2004). Accordingly, we adapted existing methods to measure the VLCFA-containing ceramide moiety of sphingolipids. Wild-type kernels accumulate approximately 2.8 µmol ceramides g^{-1}, which accounts for approximately 5% of the fatty acids present in this organ (Figure 9c). Over 95% of these ceramides contain 4,8-Sphingadienine as the long-chain base. As expected, the vast majority (approximately 85%) of these fatty acids are hydroxylated and approximately half are VLCFAs of 20–26 carbons (Figure S8a; Table S5). The *gl8a* mutation reduces the accumulation of ceramides to approximately 10% of wild-type levels (0.31 versus 2.8 µmol g^{-1}; Figure 9c), but does not significantly affect the ratio of <20C fatty acids to VLCFAs (Figure 9c), nor does it significantly affect the fatty acid composition of ceramides (Figure S8a; Table S5). In contrast, although the *gl8b* single mutant does not significantly affect the total accumulation of ceramides (3.3 versus 2.8 µmol g^{-1}; Figure 9c), it does affect the fatty acid composition of ceramides. Specifically, the kernel ceramides (Figure S8; Table S5) from *gl8b* mutants contain a relatively high proportion (27 mol %) of a novel fatty acid, hydroxypalmitate (16h:0) that is undetectable in the ceramides from wild type and *gl8a* kernels. The accumulation of the ceramide-associated 18h:0 fatty acid also increases in the *gl8b* mutant kernels. These increases occur at the expense of the ceramide-associated 18:0 and 18h:1 fatty acids, which accumulate to lower levels in the *gl8b* mutant relative to both wild type and *gl8a* kernels. Because the two single mutants express distinct chemotypes, we conclude that *gl8a* and *gl8b* have only partially redundant functions.

A separate experiment was conducted to determine the effect of the *gl8a*, *gl8b* double mutant on the accumulation of

fatty acids and ceramides. In this experiment kernels resulting from the self-pollination of a plant homozygous for *gl8b* and heterozygous for *gl8a* were genotyped (Experimental procedures). The fatty acid composition of kernels homozygous for both *gl8a* and *gl8b* (i.e., *gl8a*, *gl8b* double mutants) were compared with kernels homozygous for wild-type and mutant alleles of the *gl8a* and *gl8b* loci, respectively (i.e., *gl8b* single mutants). The fatty acid compositions of these kernels are presented in Figure S7b and Table S6. In this experiment the *gl8a*, *gl8b* double mutant kernels accumulated significantly less VLCFAs than the *gl8b* single mutants (0.3 versus 2.0 μmol VLCFAs g^{-1}, Figure 9b). As in the previous experiment, the accumulation of ceramides was also determined. In this experiment, *gl8a*, *gl8b* double mutant kernels accumulated significantly less ceramide than the *gl8b* single mutants (0.63 versus 3.6 μmol ceramides g^{-1}, Figure 9d; Table S7). Despite the dramatic reduction in the accumulation of ceramides in the *gl8a*, *gl8b* double mutant relative to the *gl8b* single mutant, relative to wild type the *gl8b* single mutant and the *gl8a*, *gl8b* double mutant both exhibited an increased accumulation of 16h:0 and 18h:0 ceramides and a decreased accumulation of 18:0 and 18h:1 ceramides (Figure S8).

Because the genetic backgrounds of the two experiments described in Figure 9(a,c) versus 9(b,d) differed, it is not appropriate to directly compare their results. Even so, it is puzzling to note that the accumulation of VLCFAs and ceramides in the *gl8a*, *gl8b* double mutant is similar to that of the *gl8a* single mutant, yet only the former is lethal.

Discussion

Maize contains two genes that encode KCR

3-Ketoacyl reductase is one of four enzymes required for the elongation of fatty acids to generate the VLCFAs that serve as precursors to the biosynthesis of a wide range of compounds, including cuticular waxes. In maize, two genes (*gl8a* and *gl8b*) encode KCR. Sequence analyses of genomic and cDNA clones for these genes reveal that their gene structures are conserved and that the proteins they encode are 97% identical. Genetic mapping experiments have placed *gl8a* and *gl8b* on syntenic chromosomal regions. Syntenic regions are believed to be the result of an ancient segmental allotetraploidization event that occurred approximately 20.5 million years ago (Ma) during the evolution of maize (Gaut and Doebley, 1997; Helentjaris *et al.*, 1988). The extreme degree of nucleotide identity (96%) that exists between these two genes is, however, inconsistent with a divergence time of more than 20 Ma. The time of divergence between *gl8a* and *gl8b* was calculated using the synonymous distance estimate of 0.0265 and the estimated synonymous substitution rate of 5×10^{-9} to 30×10^{-9} substitutions per site per year (Wolfe *et al.*, 1987) to yield a divergence time of between 0.44 and 2.65 Ma. The upper limit of this estimate is substantially more recent than the 11.4 Ma estimate of interspecific hybridization and transition to disomy in maize (Gaut and Doebley, 1997). The Arabidopsis genome contains two *gl8a* homologs (Genbank accession U89512 and NM_102292) located in a region that is part of a segmental duplication (Redundancy Viewer at http://mips.gsf.de/proj/thal/db/gv/rv/rv_frame.html). However, these duplicate genes exhibit only 63% nucleotide identity and encode proteins that are only 59% similar. The very recent divergence of *gl8a* and *gl8b* in maize coupled with the low similarity between the duplicate *gl8* homologs of Arabidopsis suggests that the maize *gl8* genes participated in a recent gene conversion-like event. Consistent with this hypothesis is the finding that nucleotide identity outside of the maize paralogs is substantially lower than within the introns of *gl8a* and *gl8b*. Such a gene conversion-like event is also thought to be the cause for the low level of divergence between the duplicate *adh* genes of rice (Gaut *et al.*, 1999).

Regardless of their origins, duplicate genes have three primary fates: (i) decay through mutation resulting in a pseudogene; (ii) functional divergence; or (iii) retention of the original, or similar, gene functions (reviewed by Wendel, 2000). The isolation of *gl8b* cDNAs indicates that *gl8b* is indeed expressed and thus is not a pseudogene. Functional divergence can reflect differences in expression and/or biochemical specificity. RNA gel-blot, transgenic, and *in situ* analyses consistently indicate that although *gl8a* is expressed at higher levels than *gl8b*, these two paralogs have very similar expression patterns. Although these genes have not diverged in terms of their expression patterns, they may have different biochemical specificities. For example, the two proteins might be involved in the elongation of fatty acids destined to be incorporated into different wax constituents. Alternatively, they could also be involved in the elongation of fatty acids destined for incorporation into the same constituents, but have different acyl chain length specificities. This specificity could be the result of either catalytic differences between the proteins *per se*, or a consequence of differential affinities for fatty acid elongase systems that have different substrate specificities. In any of these cases, mutations in these two genes would be expected to confer different metabolic phenotypes.

GL8A and GL8B have at least partially redundant biochemical functions

Mutations in either of the *gl8* paralogs reduce the total accumulation of cuticular waxes and condition similar changes in the composition of the most abundant components of seedling cuticular waxes, that is, in alcohols and aldehydes. The magnitude of the effects of the *gl8a* and *gl8b* mutations parallels the expression levels of these genes, that is, mutations in the more highly expressed *gl8a* gene reduce cuticular wax accumulation by 94%, whereas the

gl8b mutation reduces cuticular wax accumulation by only 45%. Similarly, *gl8a* mutants have more dramatic effects on the proportion of short-chain alcohols and aldehydes than does the *gl8b* mutant. These differences probably account for the fact that *gl8a* mutants, but not the *gl8b* mutant, present a glossy phenotype. Hence, based on the similarity of the proteins encoded by these genes, their very similar expression patterns, and the similar effects their mutants have on cuticular wax composition, it appears that *gl8a* and *gl8b* have at least partially redundant functions in cuticular wax biosynthesis.

In contrast, the single mutants do have some differential effects on the composition of some minor constituents of cuticular waxes. For example, the *gl8b* mutant, but not *gl8a* mutants, conditions an increased accumulation of esters and reduces the accumulation of ketones to undetectable levels. These finding may suggest that the two genes are not entirely redundant. However, because these differences affect minor wax constituents, genetic variation between the *gl8a* and *gl8b* mutant lines may have contributed to these latter observations.

The GL8 proteins are involved in the elongation of fatty acids used by both the reduction and decarbonylation pathways

Consistent with the role of the GL8 protein in acyl chain elongation, mutations in either *gl8* gene reduce the carbon chain lengths of juvenile wax components. In maize, the reduction and decarbonylation pathways utilize 32C aldehydes that are either reduced to alcohols (reduction) or decarbonylated to 31C alkanes (decarbonylation). Previous analyses have been interpreted to suggest that distinct elongases synthesize separate pools of aldehydes for these two pathways (Vioque and Kolattukudy, 1997). Consistent with this view, we found that the chain length of the aldehyde pool which is reduced to alcohols is greatly affected by the *gl8* mutation, but the chain length of the pool, which undergoes decarbonylation to generate alkanes, appears not to be greatly affected by the *gl8* mutation. However, the *gl8a* and *gl8b* single mutants similarly affect the total accumulation of products from both the reduction and decarbonylation pathways. Hence, we conclude that the ketoreductase encoded by *gl8a* and *gl8b* supplies VLCFAs to both pools of aldehydes.

gl8a *and* gl8b *double mutants cause lethality during embryo development*

The finding that the *gl8a*, *gl8b* double mutant is lethal during seed development indicates that these two genes encode an overlapping physiological function that is essential during seed development. Given that these genes encode components of fatty acid elongase, this finding suggests that VLCFAs are essential, which is consistent with earlier observations that cafenstrole, an inhibitor of fatty acid elongation, is toxic to some plant species (Takahashi *et al.*, 2001). The observation that the non-viable *gl8a*, *gl8b* double mutant kernels lack embryos and scutella, but develop normal endosperms and pericarps, indicates that the function associated with these two genes is essential in the kernel only during the development of the former two organs. This is consistent with the finding that these two genes are expressed to high levels in the embryo axes and scutella of germinating kernels.

The finding that a *gl8a*- and *gl8b*-associated function is essential may indicate that cuticular wax biosynthesis *per se* may be crucial for the development of the embryo and/or the scutellum. For example, cuticular waxes may be important in establishing the physical barriers between new tissues and organs as they are being laid down during embryogenesis. Thus, in the absence of both *gl8a* and *gl8b* functions, the absence of this cuticular wax barrier may be lethal during embryogenesis. Consistent with this hypothesis, a number of mutants (including certain maize *glossy* mutants) that affect normal epidermal cell development present an adherent phenotype in which emerging organs fail to physically separate, and some of these mutants are indeed lethal (Jin *et al.*, 2000; Tanaka *et al.*, 2001).

It is possible that another class of VLCFA-derived compounds is essential. Three lines of evidence suggest that *gl8a*- and *gl8b*-encoded KCR activity is required for the biosynthesis of essential VLCFA-containing components other than cuticular waxes. First, *gl8* is expressed in tissues other than those associated with cuticular wax biosynthesis (i.e., in internal tissues of the root, embryo, and leaves). Secondly, fatty acid elongase activity is found in such tissues (Schreiber *et al.*, 2000). Thirdly, the accumulation of VLCFAs is drastically reduced in double mutant kernels. The essential VLCFA-containing component(s) could include suberin, sphingolipids, and/or seed oils. However, the seed oil of maize contains only trace amounts of VLCFAs. Furthermore, mutations in the Arabidopsis *fae1* gene that encodes the seed oil-specific KCS component of the fatty acid elongase are not lethal (James *et al.*, 1995). Therefore, triacylglycerol is unlikely to be the essential VLCFA-containing compound. This leaves as potential candidates suberin and sphingolipids as the essential VLCFA-derived compound(s). An essentiality of suberin during embryo development remains to be tested.

However, the importance of sphingolipids (Lynch, 1993), which include 5% of the fatty acids of maize kernels, is indicated by the finding that the sphingolipid biosynthetic inhibitor, fumonisin, is toxic to plants (Wang *et al.*, 1996). Furthermore, yeast mutations that block the biosynthesis and accumulation of sphingolipids are lethal (Dunn *et al.*, 2004; Mandala *et al.*, 1995; Zweerink *et al.*, 1992). Hence, although *gl8a* and *gl8b* appear to be involved in the biosynthesis of the vast majority of VLCFA-containing compounds, their role in sphingolipid biosynthesis offers an

attractive hypothesis to explain the lethal phenotype associated with the double mutant. Relative to wild type, the *gl8a* single mutant, but not the *gl8b* single mutant, significantly decreases the accumulation of ceramides. On the contrary, the *gl8b* single mutant, but not the *gl8a* single mutant, alters the composition of the ceramide-associated VLCFAs. Significantly, the *gl8a*, *gl8b* double mutant shares a characteristic of the *gl8a* single mutant in that it reduces the total accumulation of ceramides. In addition, the *gl8a*, *gl8b* double mutant shares a characteristic of the *gl8b* single mutant, in that it alters the composition of the ceramide-associated VLCFAs. Hence, the *gl8a*, *gl8b* double mutant has a novel chemotype of the ceramide moiety of the sphingolipids relative to both of the single mutants. We therefore hypothesize that this novel sphingolipid chemotype is responsible for the lethality associated with the *gl8a*, *gl8b* double mutant.

Experimental procedures

Isolation of gl8b *genomic and cDNA clones*

The *gl8b* genomic clone λ5-1-1 was isolated from a λDash II (Stratagene, La Jolla, CA, USA) maize genomic library constructed by John Tossberg (Pioneer Hi-Bred International Inc., Johnston, IA, USA). The library was screened by DNA hybridization (Maniatis *et al.*, 1982) with a 0.8-kb partial *gl8a* cDNA (p88m) described by Xu *et al.* (1997). Restriction analysis of clone λ5-1-1 with *Hin*dIII and/or *Eco*RI revealed that the *gl8b* gene spans a 5.6-kb *Hin*dIII fragment and a 2.4-kb *Hin*dIII/*Eco*RI fragment. Each of these fragments was subcloned into an appropriately digested pMOB vector (Strathmann *et al.*, 1991) to generate clones gl8b5.6 and gl8b2.4, respectively. These clones were sequenced at the Iowa State University Nucleic Acid Facility on an ABI 373A automated DNA sequencer (Applied Biosystems, Foster City, CA, USA). Direct sequencing of λ DNA from clone λ5-1-1 across the *Hin*dIII junction confirmed that the two fragments are contiguous. Sequence analyses were performed using the Sequencher™ Version 3.0 software package (Gene Codes Corporation, Inc., Ann Arbor, MI, USA).

A 1.0-kb partial *gl8b* cDNA (1991-12) was isolated from a cDNA library prepared from RNA isolated from 14-day-old B73 seedling leaves by Yiji Xia using the pAD-GAL4 vector (Stratagene). This library was screened with the 0.8-kb *gl8a* cDNA clone (p88m) and both *gl8a* and *gl8b* cDNA clones were identified. The cDNAs for these genes were distinguished by amplification of their 3′-UTRs with primers g24he.p4 and gl8bsp followed by digestion of the amplified products with *Cfo*I. Products amplified from *gl8b* cDNAs do not contain the *Cfo*I restriction site while fragments amplified from *gl8a* cDNAs do. The 5′-end of the *gl8b* cDNA was isolated by 5′-RACE with 3′ nested gene-specific primers gab362 and mcd696. GeneRacer (Invitrogen, Carlsbad, CA, USA), a modified 5′-RACE procedure that allows amplification only from mRNAs having a 5′ 7-methylated guanine cap, was used to confirm that the 5′-RACE product was full length.

Constructs and probes

A 113-bp PCR product was amplified from gl8b5.6 with primers xx1128 and g13s.p2. This PCR product was cloned into the pBSK/T-vector to create the *gl8b*-specific clone 1409-4. The insert from this clone is released by digestion with *Hin*dIII and *Eco*RI. This fragment was used as the RFLP probe IAS12 to map the *gl8b* gene. The PCR product resulting from the PCR amplification of the *gl8a* cDNA clone pgl8 with primers gab457 and g24he.p5 was used as template to generate ^{32}P-labeled probe for RNA gel-blot experiments. This same PCR product was subcloned into the pCR-TOPO 4.1 vector (Invitrogen) to generate pGAB23 (clone 2490-1). Digoxigenin-labeled sense and antisense probes used for *in situ* hybridization experiments were generated from *Not*I- and *Spe*I-digested pGAB23, respectively.

RNA isolation and gel blotting

Tissue samples were collected from 7-day-old greenhouse-grown seedlings. Adult samples (leaf, husk, tassel, silk, and ear) were collected at the mid-point of anthesis. Leaf tissue was collected from the leaf attached to the primary ear. Husk, silk, and ear tissue were collected from primary ears which had been covered to prevent pollination. Husk tissue included only the innermost two or three husks. Silk tissue included silk that was both external and internal to the husks. Embryos were isolated from kernels 21 days after pollination. RNA was isolated from these tissue sources using a modified single-step acid guanidinium thiocyanate–phenol–chloroform extraction method (Chomczynski and Sacchi, 1987). Briefly, 4 g of tissue was frozen in liquid N_2 and pulverized. Fifty milliliters of denaturing reagent (38% phenol, 0.8 M guanidine thiocyanate, 0.4 M ammonium thiocyanate, 0.1 M sodium acetate, pH 5, 5% glycerol) was added and allowed to warm to RT. Samples were then heated to 60°C for 5 min before centrifugation at 12 000 ***g*** for 10 min. Supernatants were mixed with 12 ml chloroform, shaken for 15 sec, and allowed to sit at RT for 5 min before being centrifuged at 10 000 ***g*** for 10 min. The aqueous phase from each tube was mixed with 1/2 volume isopropanol and 1/2 volume 0.8 M sodium citrate/1.2 M NaCl. Samples were mixed by inverting several times and allowed to sit at RT for 10 min before centrifugation at 10 000 ***g*** for 10 min at 4°C. The RNA pellet was washed with 75% ethanol and air-dried for 1 min. RNA was resuspended in 500 μl diethyl pyrocarbonate-treated H_20 by incubating at 60°C for 10 min. RNA was quantified using a SpectraMax Plus plate reader (Molecular Devices, Sunnyvale, CA, USA). RNA was subjected to electrophoresis in a formaldehyde-containing 1.25% agarose gel and transferred to GeneScreen nylon membranes (Dupont, Boston, MS, USA). Hybridization with ^{32}P-labeled probes was conducted as described by the manufacturer.

In situ *hybridizations*

Tissue was fixed in ice-cold fixative (4% paraformaldehyde with 1% glutaraldehyde in 0.1 M phosphate-buffered saline, PBS) for 12–18 h and processed according to the protocol described by Jackson (1991). Samples were infiltrated in paraplast (Paraplast Plus; Sherwood Medical, St Louis, MO, USA) and consecutive 10-μm-thick tissue sections were cut on a Leica RM 2135 (Meyer Instruments, Houston, TX, USA) microtome and placed on ProbeOn Plus microscope slides (Fisher Scientific, Pittsburgh, PA, USA). Digoxigenin-11-UTP (DIG RNA Labeling Mix; Roche Diagnostics Indianapolis, IN, USA) was incorporated into antisense or sense RNA probes, synthesized with T7 or T3 RNA polymerase (Roche Diagnostics) according to the manufacturer's instructions. Hybridization and detection were carried out by the methods of Coen *et al.* (1990).

Generation and analysis of transgenic maize lines

The *gl8a::GUS* construct, pBKAR (clone 1608-1), was constructed by ligating the 2203-bp *Xho*I/*Xba*I fragment from the *gl8a* genomic clone, λ1512-38, into the *Xho*I and *Xba*I sites of the pDMC205 expression vector (McElroy *et al.*, 1995). The *gl8b::GUS* construct, pBBUS, was created via a two-step process that began by ligating the 2300-bp *Bgl*II/*Nco*I fragment from gl8b5.6 that had been blunt ended with S1 nuclease, into *Pvu*II-digested pDMC205 to generate clone 1339-8. To remove an out-of-frame start codon, clone 1339-8 was digested with *Sal*I and *Hin*dIII, filled in with Klenow and religated to generate pBBUS (clone 1673-11).

The Iowa State University Plant Transformation Facility generated transgenic plants carrying *gl8a::GUS* or *gl8b::GUS* from callus tissue following co-bombardment with the pBAR184(−) selection construct (Frame *et al.*, 2000). DNA samples were isolated from calli (Plant DNA Microprep Version 2.3, Dellaporta, 1994) and PCR analyses performed to identify those that contained complete transgenes. Calli transformed with *gl8a::GUS* were PCR amplified with primer pairs cdsp6-2/gl8a55; gl8a57/gl8a51; xx1128/gus-4; and gus-1/nos3p. Calli transformed with *gl8b::GUS* primers were amplified with cdsp6-2/g13s.p3; g13s.p1/gus-3 and gus1/nos3p. Fourteen independently derived calli transformed with *gl8a::GUS* and 11 calli transformed with *gl8b::GUS* were regenerated into plants. Transgenic lines were propagated by outcrossing. BAR resistance was monitored either by spraying 7-day-old seedlings with 0.2% Liberty (AgrEvo, Wilmington, DE, USA) or dipping adult leaves in 0.5% Liberty.

The expression of GUS in transgenic plants was monitored by tissue sections in GUS assay buffer (50 mM sodium phosphate buffer, pH 7.0, 10 mM EDTA, 0.1% Triton X-100, 2 mM potassium ferrocyanide, 2 mM potassium ferricyanide, 100 μg ml^{-1} chloramphenicol, 1 mg ml^{-1} X-Gluc) at 37°C for 12–18 h and then clearing samples with 70% ethanol. Five of the 14 *gl8a::GUS*-containing transgenic lines (p2p14-2, p2p14-19, p2p14-20, p2p14-23, and p2p14-35) and four of the 11 *gl8b::GUS*-containing transgenic lines (p2p24-1, p2p24-5, p2p24-14, and p2p24-25) exhibited high levels of GUS expression. The patterns of GUS expression among these lines were very similar. Two of the *gl8a::GUS*-containing transgenic lines (p2p14-7 and p2p14-55) and one of the *gl8b::GUS*-containing transgenic lines (p2p24-31) exhibited low levels of GUS activity. The GUS expression patterns of these lines were not extensively analyzed. The remainder of the lines did not stably express GUS activity.

Genetic stocks

All of the *gl8a* mutant alleles used in this study, including the deletion allele, were described by Dietrich *et al.* (2002). The *gl8a* alleles used in this study are available from the Maize Genetics Stock Center. The *gl8a-Mu 77-3134* samples used for wax analyses were from F_2 seedlings obtained from a stock (01-4375 self) that had been previously backcrossed to the inbred line B73 five times. The *gl8b* mutant allele *gl8b-Mu* BT94-149 was identified from a PCR-based TUSC screen performed by Robert Meeley (Pioneer Hi-Bred International, Inc.). A Material Transfer Agreement governs the distribution of this stock; inquires should be directed to Dr Meeley. The *gl8b-Mu BT94-149* seedlings used for wax analyses were obtained by self-pollinating a stock (01-4373 self) homozygous for *gl8b-Mu BT94-149* that had been previously backcrossed into the inbred B73 one time. The *gl8a gl8b* double mutant seedlings used for lipid analyses were obtained via the self-pollination of a stock (02-2488-1 self) homozygous for *gl8b-Mu BT94-149* and heterozygous for *gl8a-Mu 88-3142*. This stock was created by initially crossing together *gl8a*- and *gl8b*-containing stocks that had been backcrossed to B73 five and two times, respectively.

Genotyping gl8b

High-throughput DNA isolations were performed as described by Dietrich *et al.* (2002). Endosperm DNA was isolated from imbibed kernels (after removal of the maternally derived pericarp) using Gentra (Minneapolis, MN, USA) Puregene DNA isolation kit (cat. no. D-5000A). Plants homozygous for *gl8b* were identified by PCR amplification with two primer pairs: gl8b-a in conjunction with Mu-TIR, and gl8b-c in conjunction with 8bm225. Primer 8bm225 is an IDP primer that amplifies *Gl8b-B73*, but not *gl8b-Mu BT94-149*. Thus, the primer pair gl8b-c/8bm225 does not produce a PCR amplification product from template DNA isolated from plants homozygous for *gl8b-Mu BT94-149*. The presence of the *gl8b-Mu BT94-149* allele was confirmed via amplification with primer pair gl8b-a and the Mu TIR-specific primer, Mu-TIR.

PCR primers

8bm225: 5′ GGA ATT TGT TGA GAG TCA TTG
cdsp6-2: 5′ GCT ATT TAG GTG ACA CTA TA G
g13s.p1: 5′ AAT CCC TCC TCC CCA CCT GAC C
g13s.p2: 5′ CTG GTC GAT GCG GTG CGG TGT C
g13s.p3: 5′ GAA GAC AGC AGC AGC GGC AGA
g24he.p4: 5′ CCT ATG CTC GTG CTG CCG TTC GTC
g24he.p5: 5′ CCT ATG CTC GTG CTG CCG TTC GTC
gab362: 5′ AGT CCT TGA GCG CCT CGA C
gab457: 5′ GGT GGA CGA GGA GCT GAT G
gl8a51: 5′ TGT GCC TGC CCC TGT GTC
gl8a55: 5′ CTT CTT CCT CCA GCA TTC
gl8a57: 5′ CGG CTC GCT TCT CTC CAC TAC
gl8b-a: 5′ GCC ACG GTT CGT CTG CAA AAC ACT G
gl8b-c: 5′ GCA TCC TTG GCT ATT TAC TGG CTC GGT T
gl8bsp: 5′ CCG TGG ATG GAG CAA TGG
gus-1: 5′ AAA CCC CAA CCC GTG AAA
gus-3: 5′ ACC CAC ACT TTG CCG TAA TG
gus-4: 5′ ATA TCT GCA TCG GCG AAC TG
mcd696: 5′ CGC ACC TCG GGG ACC TTG G
Mu-TIR: 5′ AGA GAA GC C AAC GCC A(AT)C GCC TC(CT) ATT TCG TC
nos3p: 5′ AAG ACC GGC AAC AGG ATT C
xx1128: 5′ TCT GTT CGT GTT CGG TTA GTC TTG

Microscopy

Scanning electron microscopy was performed at the Iowa State University Bessey Microscopy Facility on the adaxial surface of the second leaf from 10-day-old seedlings. Freshly harvested samples were coated with a 60/40 palladium/gold alloy using a Denton (Moorestown, NJ, USA) Vacuum Desk II LC sputter/etch unit and analyzed with a Jeol scanning electron microscope (model 5800 LV; Tokyo, Japan).

Chemical analyses

Cuticular waxes were extracted from 9- to 10-day-old maize seedlings grown in greenhouse sand benches. Prior to extraction, the coleoptile was removed from the seedlings, and 1 μg of the internal standard (hexadecane; Sigma Chemical Co., St Louis, MO,

USA) was applied to the leaves. The leaves were then immersed in HPLC-grade chloroform for 60 sec. The extract was then filtered with glass wool. Plant material was then dried overnight at 100°C and weighed. The filtered extract was taken to dryness under reduced pressure using a rotary evaporator at 30°C. The dried wax was dissolved in a small volume of chloroform and subjected to GC-MS analysis. GC-MS chromatographic analysis was conducted using a Gas Chromatograph (6890 series; Agilent, Palo Alto, CA, USA), equipped with a Mass Detector 5973 (Agilent). Wax constituents were separated on a 30 m long, 0.32 mm i.d. fused silica capillary column (HP-1) using He as a carrier gas. The injector and detector were held at 325°C. The 80°C oven was heated at a rate of 5°C min^{-1} up to 260°C. This temperature was maintained for 10 min, and then elevated at 5°C min^{-1} to 320°C and held at this final temperature for 30 min. Identification of the wax components was facilitated by using HP enhanced ChemStation ™ G1701 BA version B.01.00 with Windows NT ™ operating system (Agilent).

Ester isomers with the same total carbon number, but differing in their acid and alcohol moieties, were identified via the characteristic protonated acid fragmentation ion obtained via electron-impact mass spectrometry (Reiter *et al.*, 1999).

To quantify the accumulation of different cuticular wax components, the response of the mass-spectrometer was calibrated for each component class relative to the hexadecane internal standard using an FID detector. For this purpose the following commercially available standards (Sigma Chemical Co.) were used (the response of the mass-spectrometer relative to hexadecane is provided in brackets). Specifically, 1-octacosanol was the alcohol standard (93% of the hexadecane response), decanal was the aldehyde standard (86% of the hexadecane response), heptacosane was the alkane standard (98% of the hexadecane response), 6-tricosanone was the ketone standard (85% of the hexadecane response), and icosyl docosanate was the ester standard (72% of the hexadecane response).

The total fatty acid content of plant material was determined by first acid-hydrolyzing all fatty acid-containing compounds, and subsequently recovering and quantifying the released fatty acids as methyl esters by GC-MS. Maternal pericarp tissue was removed from kernels prior to analysis. An aliquot of a known weight (between 30 and 40 mg) of powdered kernels, spiked with 10 μg of nonadecanoic acid as an internal standard, was homogenized in a Ten-Broek homogenizer with about 1 ml of PBS. The extract was adjusted to a final concentration of 6 N HCl, by the addition of concentrated acid. Following a 6-h incubation at 90°C, the hydrolyzed fatty acids were recovered by extraction with hexane and converted to their methyl esters. Fatty acid methyl esters were analyzed with a GC-MS, using the same column and chromatographic conditions used to analyze cuticular wax components, except that the oven temperature was initially at 80°C and then heated at a rate of 5°C min^{-1} to 200°C. This temperature was maintained for 10 min, and then elevated at 5°C min^{-1} to 260°C and held at this final temperature for 10 min.

To analyze the ceramide moiety of sphingolipids, powdered kernels (minus pericarps) were extracted according to the protocol of Sullards and Merrill (2001). An accurately weighed aliquot of kernel powder (of approximately 0.02–0.5 g), spiked with 0.5 nmol of C17 ceramide (dissolved in ethanol; Avanti Polar Lipids Inc., Alabaster, AL, USA), was homogenized in a Ten-Broek homogenizer with about 0.5 ml of PBS and 0.5 ml of methanol. The extract was sonicated for 30 sec and incubated at 48°C overnight. To the cooled extract, 100 μl of 1 M KOH in methanol was added, sonicated for 30 sec, and saponified by incubation at 37°C for 2 h. The solution was then neutralized with glacial acetic acid and 3 ml of chloroform/H_2O (1:2, v/v) was added and the mixture was vortexed. Phases were separated by centrifugation for 10 min and the lower organic phase containing the ceramides was recovered and concentrated by evaporation under a stream of N_2 gas. The dried sample was dissolved in 1 ml of HPLC grade acetonitrile, and silylated by incubating at 70°C for 20 min after the addition of 70 μl of *N,O*-Bis(trimethyl-silyl)trifluoroacetamide containing 1% trimethylchlorosilane (Sigma Chemical Co.). After evaporating the excess reagents under a stream of N_2 gas, the silylated sample was dissolved in hexane for GC-MS analysis. GC was performed with a 30 m long, 0.32 mm i.d., fused silica capillary column (HP-5; Agilent). Ceramides were identified and analyzed by their characteristic mass-spectrum as described in Raith *et al.* (2000).

Acknowledgements

We thank Dr Ben Burr (Brookhaven National Laboratory, Upton, NY) for analyzing mapping data for IAS12 and Dr Tom Peterson (Iowa State University) for discussions of GUS staining patterns. Xiaojie Xu isolated clone *gl8b* λ5-1-1; Marianne Smith performed the *in situ* hybridization experiments. This research was supported in part by grants from the National Science Foundation (IBN-9808559, IBN-0344852 and IOB-0344852) to P.S.S. and B.J.N. and by Hatch Act and State of Iowa funds. C.R.D. was funded in part by a USDA National Needs Fellowship in Plant Biotechnology.

Supplementary Material

The following material is available from http://www.blackwellpublishing.com/products/journals/suppmat/TPJ/TPJ2418/TPJ2418sm.htm

Figure S1. Free alcohols.
Figure S2. Aldehydes.
Figure S3. Alkanes.
Figure S4. Ketones.
Figure S5. Free acids.
Figure S6. Esters.
Figure S7. (a, b) Total fatty acid composition of kernels.
Figure S8. Fatty acid composition of kernel ceramides.
Table S1 Cuticular wax composition (nmol g^{-1} dry weight)
Table S2 Esters of cuticular waxes (nmol g^{-1} dry weight)
Table S3 Carbon chain length of all cuticular wax components (μmol g^{-1} dry weight)
Table S4 Fatty acid composition of *gl8* mutant kernels (μmol g^{-1} dry weight)
Table S5 Ceramide-associated fatty acid of *gl8* mutant kernels (μmol g^{-1} dry weight)
Table S6 Fatty acid composition of *gl8a*, *gl8b* double mutant kernels (μmol g^{-1} dry weight)
Table S7 Ceramide-associated fatty acid of *gl8a*, *gl8b* double mutant kernels (μmol g^{-1} dry weight)

References

Andersson, H., Kappeler, F. and Hauri, H.P. (1999) Protein targeting to endoplasmic reticulum by dilysine signals involves direct retention in addition to retrieval. *J. Biol. Chem.* **274**, 15080–15084.

Barret, P., Delourme, R., Renard, M., Domergue, F., Lessire, R., Delseny, M. and Roscoe, T.J. (1998) A rapeseed *FAE1* gene is linked to the *E1* locus associated with variation in the content of erucic acid. *Theor. Appl. Genet.* **96**, 177–186.

Beaudoin, F., Gable, K., Sayanova, O., Dunn, T. and Napier, J.A. (2002) A *Saccharomyces cerevisiae* gene required for heterologous fatty acid elongase activity encodes a microsomal beta-keto-reductase. *J. Biol. Chem.* **277**, 11481–11488.

Beisson, F., Koo, A.J., Ruuska, S. *et al.* (2003) Arabidopsis genes involved in acyl lipid metabolism. A 2003 census of the candidates, a study of the distribution of expressed sequence tags in organs, and a web-based database. *Plant Physiol.* **132**, 681–697.

Bensen, R.J., Johal, G.S., Crane, V.C., Tossberg, T.J., Schnable, P.S., Meeley, R.B. and Briggs, S.P. (1995) Cloning and characterization of the maize *An1* gene. *Plant Cell*, **7**, 75–84.

Bianchi, G., Avato, P. and Salamini, F. (1979) Glossy mutants of maize. IX. Chemistry of *glossy 4*, *glossy 8*, *glossy 15* and *glossy 18* surface waxes. *Heredity*, **42**, 391–395.

Bianchi, A., Bianchi, G. and Avato, P. (1985) Biosynthetic pathways of epicuticular wax of maize as assessed by mutation, light, plant age and inhibitor studies. *Maydica*, **30**, 179–198.

Bligh, E.G. and Dyer, W.J. (1959) A rapid method of total extraction and purification. *Can. J. Biochem. Physiol.* **37**, 911–917.

Burr, B. and Burr, F. (1991) Recombinant inbreds for molecular mapping in maize: theoretical and practical considerations. *Trends Genet.* **7**, 55–61.

Chomczynski, P. and Sacchi, N. (1987) Single-step method of RNA isolation by acid guanidinium thiocyanate-phenol-chloroform extraction. *Anal. Biochem.* **162**, 156–159.

Coe, E.H. (1993) Gene list and working maps. *Maize Genet. Coop. Newsl.* **67**, 133–166.

Coen, E.S., Doyle, J.M., Elliott, R., Murphy, G. and Carpenter, R. (1990) *floricaula*: A homeotic gene required for flower development in *Antirrhinum majus*. *Cell*, **63**, 1311–1322.

Dellaporta, S. (1994) Plant DNA miniprep and microprep versions 2.1–2.3. In *The Maize Handbook* (Freeling, M. and Walbot, V. eds). New York: Springer-Verlag, pp. 522–525.

Devos, K.M. and Gale, M.D. (1997) Comparative genetics in the grasses. *Plant Mol. Biol.* **35**, 3–15.

Dietrich, C.R., Cui, F., Packila, M.L., Li, J., Ashlock, D.A., Nikolau, B.J. and Schnable, P.S. (2002) Maize *Mu* transposons are targeted to the 5′ UTR of the *gl8* gene and sequences flanking *Mu* target site duplications throughout the genome exhibit non-random nucleotide composition. *Genetics*, **160**, 697–716.

Domergue, F., Bessoule, P., Moreau, R., Lessire, C. and Cassagne, C. (1998) Plant lipid biosynthesis. In *Fundamental and Agricultural Applications* (Harwood, J.L., ed.). Cambridge, UK: Cambridge University Press, pp. 185–222.

Domergue, F., Chevalier, S., Santarelli, X., Cassagne, C. and Lessire, R. (1999) Evidence that oleoyl-CoA and ATP-dependent elongations coexist in rapeseed (*Brassica napus* L.). *Eur. J. Biochem.* **263**, 464–470.

Doseff, A., Martienssen, R. and Sundaresan, V. (1991) Somatic excision of the *Mu1* transposable element of maize. *Nucleic Acids Res.* **19**, 579–584.

Dunn, T.M., Lynch, D.V., Michaelson, L.V. and Napier, J.A. (2004) A post-genomic approach to understanding sphingolipid metabolism in *Arabidopsis thaliana*. *Ann. Bot. (Lond)* **93**, 483–497.

Eigenbrode, S.D. and Espelie, K.E. (1995) Effects of plant epicuticular lipids on insect herbivores. *Annu. Rev. Entomol.* **40**, 171–194.

Eigenbrode, S.D. and Shelton, A.M. (1990) Behavior of neonate diamondback moth larvae (*Lepidoptera: Plutellidae*) on glossy-leafed resistant *Brassica oleracea* L. *Environ. Entomol.* **19**, 1566–1571.

Emanuelsson, O., Nielsen, H., Brunak, S. and von Heijne, G. (2000) Predicting subcellular localization of proteins based on their N-terminal amino acid sequence. *J. Mol. Biol.* **300**, 1005–1016.

Emerson, R.A., Beadle, G.W. and Fraser, A.C. (1935) A summary of linkage studies in maize. *Cornell Univ. Agric. Exp. Stn Mem.* **180**, 1–83.

Ensor, C.M. and Tai, H.H. (1991) Site-directed mutagenesis of the conserved tyrosine 151 of human placental NAD (+)-dependent 15-hydroxyprostoglandin dehydrogenase yields a catalytically inactive enzyme. *Biochem. Biophys. Res. Commun.* **176**, 840–845.

Fehling, E. and Muhkerjee, K.D. (1991) Acyl-CoA elongase from a higher plant (*Lunaria annua*): metabolic intermediates of very-long-chain acyl-CoA products and substrate specificity. *Biochim. Biophys. Acta*, **1082**, 239–246.

Fiebig, A., Mayfield, J.A., Miley, N.L., Chau, S., Fischer, R.L. and Preuss, D. (2000) Alterations in *CER6*, a gene identical to *CUT1*, differentially affect long-chain lipid content on the surface of pollen and stems. *Plant Cell*, **12**, 2001–2008.

Frame, B., Zhang, H., Cocciolone, S., Sidorenko, L.V., Dietrich, C.R., Pegg, S.E., Zhen, S., Schnable, P.S. and Wang, K. (2000) Production of transgenic maize from bombarded type II callus: effect of gold particle size and callus morphology on transformation efficiency. *In Vitro Cell Dev. Biol. Plant*, **36**, 21–29.

Gable, K., Garton, S., Napier, J.A. and Dunn, T.M. (2004) Functional characterization of the *Arabidopsis thaliana* orthologue of Tsc13p, the enoyl reductase of the yeast microsomal fatty acid elongating system. *J. Exp. Bot.* **55**, 543–545.

Gaut, B.S. and Doebley, J.F. (1997) DNA sequence evidence for the segmental allotetraploid origin of maize. *Proc. Natl Acad. Sci. USA*, **94**, 6809–6814.

Gaut, B.S., Peek, A.S., Morton, B.R. and Clegg, M.T. (1999) Patterns of genetic diversification within the *Adh* gene family in the grasses (*Poaceae*). *Mol. Biol. Evol.* **16**, 1086–1097.

Helentjaris, T., Weber, D. and Wright, S. (1988) Identification of the genomic locations of duplicate nucleotide sequences in maize by analysis of restriction fragment length polymorphisms. *Genetics*, **118**, 353–363.

Jackson, D. (1991) *In situ* hybridization in plants. In *Molecular Plant Pathology* (Gurr, S.J., McPherson, M.J. and Bowles, D.J., eds). New York: Oxford University Press, pp. 163–174.

Jackson, M.R., Nilsson, T. and Peterson, P.A. (1990) Identification of a consensus motif for retention of transmembrane proteins in the endoplasmic reticulum. *EMBO J.* **9**, 3153–3162.

James, D.W., Jr, Lim, E., Keller, J., Plooy, I., Ralston, E. and Dooner, H.K. (1995) Directed tagging of the *Arabidopsis FATTY ACID ELONGATION* (*FAE1*) gene with the maize transposon *Activator*. *Plant Cell*, **7**, 309–319.

Jenks, M.A., Joly, R.J., Peters, P.J., Rich, P.J., Atell, J.D. and Ashworth, E.N. (1994) Chemically induced cuticle mutation affecting epidermal conductance to water vapor and disease susceptibility in *Sorghum bicolor* (L.) Moench. *Plant Physiol.* **105**, 1239–1245.

Jin, P., Guo, T. and Becraft, P.W. (2000) The maize CR4 receptor-like kinase mediates a growth factor-like differentiation response. *Genesis*, **27**, 104–116.

Kiesselbach, T.A. (1949) *The Structure and Reproduction of Corn* (50th Anniversary edition 1999). New York: Cold Spring Harbor Laboratory.

Kohlwein, S.D., Eder, S., Oh, C.S., Martin, C.E., Gable, K., Bacikova, D. and Dunn, T. (2001) Tsc13p is required for fatty acid elongation and localizes to a novel structure at the nuclear-vacuolar interface in *Saccharomyces cerevisiae*. *Mol. Cell Biol.* **21**, 109–125.

Kolattukudy, P.E. (1981) Structure, biosynthesis, and biodegradation of cutin and suberin. *Annu. Rev. Plant Physiol.* **32**, 539–567.

Kolattukudy, P.E. (1987) Lipid-derived defense polymers and waxes and their role in plant–microbe interaction. In *The Biochemistry of Plants* (Stumpf, P.K., ed.). New York: Academic Press, pp. 291–314.

Lassner, M.W., Lardizabal, K. and Metz, J.G. (1996) A jojoba beta-ketoacyl-CoA synthase cDNA complements the canola fatty acid elongation mutation in transgenic plants. *Plant Cell*, **8**, 281–292.

Lessire, R., Bessoule, J.J. and Cassagne, C. (1985) Solubilization of C18-CoA and C20-CoA elongases from *Allium porrum* L. epidermal cell microsomes. *FEBS Lett.* **187**, 314–320.

Lynch, D.V. (1993) Sphingolipids. In *Lipid Metabolism in Plants* (Moore, T.S., ed.). Boca Raton: CRC Press, pp. 285–308.

Mandala, S.M., Thornton, R.A., Frommer, B.R., Curotto, J.E., Rozdilsky, W., Kurtz, M.B., Giacobbe, R.A., Bills, G.F., Cabello, M.A. and Martin, I. (1995) The discovery of australifungin, a novel inhibitor of sphinganine N-acyltransferase from *Sporormiella australis*. Producing organism, fermentation, isolation, and biological activity. *J. Antibiot. (Tokyo)* **48**, 349–356.

Maniatis, T., Fritsch, E.F. and Sambrook, J. (1982) *Molecular Cloning, A Laboratory Manual*. New York: Cold Spring Harbor Laboratory.

Martin, J.T. and Juniper, B.E. (1970) *The Cuticle of Plants*. Edinburgh: Edward Arnold Ltd.

McElroy, D., Chamberlin, D.A., Moon, E. and Wilson, K.J. (1995) Development of *gusA* reporter gene constructs for cereal transformation: availability of plant transformation vectors from the CAMBIA Molecular Genetic Resource Service. *Mol. Breed.* **1**, 27–37.

Millar, A.A., Clemens, S., Zachgo, S., Giblin, E.M., Taylor, D.C. and Kunst, L. (1999) *CUT1*, an *Arabidopsis* gene required for cuticular wax biosynthesis and pollen fertility, encodes a very-long-chain fatty acid condensing enzyme. *Plant Cell*, **11**, 825–838.

Nakai, K. and Kanehisa, M. (1992) A knowledge base for predicting protein localization sites in eukaryotic cells. *Genomics*, **14**, 897–911.

Nielsen, H., Engelbrecht, J., Brunak, S. and von Heijne, G. (1997) Identification of prokaryotic and eukaryotic signal peptides and prediction of their cleavage sites. *Protein Eng.* **10**, 1–6.

Post-Beittenmiller, D. (1996) Biochemistry and molecular biology of wax accumulation in plants. *Annu. Rev. Plant Physiol.* **47**, 405–430.

Preuss, D., Lemieux, B., Yen, G. and Davis, R.W. (1993) A conditional sterile mutation eliminates surface components from *Arabidopsis* pollen and disrupts cell signaling during fertilization. *Genes Dev.* **7**, 974–985.

Raith, K., Darius, J. and Neubert, R.H.H. (2000) Ceramide analysis utilizing gas chromatography-mass spectrometry. *J. Chromatogr. A.* **876**, 229–233.

Reicosky, D.A. and Hanover, J.W. (1978) Physiological effects of surface waxes. I. Light reflectance for glaucous and nonglaucous *Picea pungens*. *Plant Physiol.* **62**, 101–104.

Reiter, B., Lechner, M., Lober, E. and Aichholz, R. (1999) Isolation and characterization of wax esters in fennel and caraway seed oil by SPE-GC. *J. High Resolut. Chromatogr.* **22**, 514–520.

Schnable, P.S., Stindard, P.S., Wen, T.J., Heinen, S., Weber, D., Schneerman, M., Zhang, L., Hansen, J.D. and Nikolau, B.J. (1994) The genetics of cuticular wax biosynthesis. *Maydica*, **39**, 279–287.

Schreiber, L., Skrabs, M., Hartmann, K., Becker, D., Cassagne, C. and Lessire, R. (2000) Biochemical and molecular characterization of corn (*Zea mays* L.) root elongases. *Biochem. Soc. Trans.* **28**, 647–649.

Stinard, P.S. and Schnable, P.S. (1993) Four-point linkage data for *ae pr lw2 gl8* on 5L. *Maize Genet. Coop. Newsl.* **67**, 8–9.

Strathmann, M., Hamilton, B.A., Mayeda, C.A., Simon, M.I., Meyerowitz, E.M. and Palazzolo, M. (1991) Transposon-facilitated DNA sequencing. *Proc. Natl Acad. Sci. USA*, **88**, 1247–1250.

Sullards, M.C. and Merrill, A.H. (2001) Analysis of sphingosine 1-phosphate, ceramides, and other bioactive sphingolipids by high-performance liquid chromatography-tandem mass spectrometry. *Sci STKE.* **67**, PL1.

Takahashi, H., Ohki, A., Kanzaki, M., Tanaka, A., Sato, Y., Matthes, B., Boger, P. and Wakabayashi, K. (2001) Very-long-chain fatty acid biosynthesis is inhibited by cafenstrole, N,N-diethyl-3-mesitylsulfonyl-1H-1,2,4-triazole-1-carboxamide and its analogs. *Z. Naturforsch*, **56**, 781–786.

Tanaka, H., Onouchi, H., Kondo, M., Hara-Nishimura, I., Nishimura, M., Machida, C. and Machida, Y. (2001) A subtilisin-like serine protease is required for epidermal surface formation in *Arabidopsis* embryos and juvenile plants. *Development*, **128**, 4681–4689.

Todd, J., Post-Beittenmiller, D. and Jaworski, J.G. (1999) KCS1 encodes a fatty acid elongase 3-ketoacyl-CoA synthase affecting wax biosynthesis in *Arabidopsis thaliana*. *Plant J.* **17**, 119–130.

Trenkamp, S., Martin, W. and Tietjen, K. (2004) Specific and differential inhibition of very-long-chain fatty acid elongases from *Arabidopsis thaliana* by different herbicides. *Proc. Natl Acad. Sci. USA*, **101(32)**, 11903–11908.

Vioque, J. and Kolattukudy, P.E. (1997) Resolution and purification of an aldehyde-generating and an alcohol-generating fatty acyl-coa reductase from pea Leaves (*Pisum sativum* L.). *Arch. Biochem. Biophys.* **340**, 64–72.

Wang, H., Li, J., Bostock, R.M. and Gilchrist, D.G. (1996) Apoptosis: a functional paradigm for programmed plant cell death induced by a host-selective phytotoxin and invoked during development. *Plant Cell*, **8**, 375–391.

Wen, T.J. and Schnable, P.S. (1994) Analyses of mutants of three genes that influence root hair development in *Zea mays* (Gramineae) suggest that root hairs are dispensable. *Am. J. Bot.* **81**, 833–842.

Wendel, J.F. (2000) Genome evolution in polyploids. *Plant Mol. Biol.* **42**, 225–249.

von Wettstein-Knowles, P. (1982) Elongase and epicuticular wax biosynthesis. *Physiol. Veg.* **20**, 797–809.

von Wettstein-Knowles, P. (1987) Barley raincoats: biosynthesis and genetics. In *Plant Molecular Biology* (von Wettstein, D. and Chua, N.H., eds). New York: Plenum, pp. 305–314.

von Wettstein-Knowles, P. (1993) Waxes, cutin, and suberin. In *Lipid Metabolism in Plants* (Moore, T.S., Jr, ed.). Boca Raton: CRC Press, pp. 127–166.

Wolfe, K.H., Li, W.-H. and Sharp, P.M. (1987) Rates of nucleotide substitution vary greatly among plant mitochondrial, chloroplast, and nuclear DNAs. *Proc. Natl Acad. Sci. USA*, **84**, 9054–9058.

Xu, X., Dietrich, C.R., Delledonne, M., Xia, Y., Wen, T.J., Robertson, D.S., Nikolau, B.J. and Schnable, P.S. (1997) Sequence analysis of the cloned *glossy8* gene of maize suggests that it may code for a beta-ketoacyl reductase required for the biosynthesis of cuticular waxes. *Plant Physiol.* **115**, 501–510.

Xu, X., Dietrich, C.R., Lessire, R., Nikolau, B.J. and Schnable, P.S. (2002) The endoplasmic reticulum-associated maize GL8 protein is a component of the acyl-CoA elongase involved in the production of cuticular waxes. *Plant Physiol.* **128**, 924–934.

Zweerink, M.M., Edison, A.M., Wells, G.B., Pinto, W. and Lester, R.L. (1992) Characterization of a novel, potent, and specific inhibitor of serine palmitoyltransferase. *J. Biol. Chem.* **15**, 25032–25038.